Directional Wavelet Bases Construction on Dyadic Quincunx Lattice

Rujie Yin, Ingrid Daubechies

September 2, 2016

Abstract

We construct directional wavelet systems in the interest of building efficient signal representation scheme with good direction selectivity. In particular, we focus on wavelet bases on dyadic quincunx lattice where dilated quincunx downsampling is used to construct orthonormal and bi-orthogonal bases and standard dyadic downsampling for low-redundancy frames. We show that the supports of both orthonormal and bi-orthogonal wavelets in our framework are discontinuous in the frequency domain. However, this irregularity constraint be avoided in frames of redundancy less than 2.

1 Introduction

In image compression and analysis, 2D tensor wavelet schemes are widely used. Despite the time-frequency localization inherited from 1D wavelet, 2D tensor wavelets suffers from poor orientation selectivity: only horizontal or vertical edges are well represented by tensor wavelets. To obtain better representation of 2D images, several directional wavelet schemes have been proposed and applied to image processing, such as directional wavelet filterbanks(DFB) and its various extensions.

Conventional DFB [1] divides the frequency domain into eight equi-angular pairs of triangles and it is critically downsampled (maximally decimated) and perfect reconstruction (PR), but without multi-resolution structure. Different approaches have been proposed to generalize DFB to multi-resolution systems, including non-uniform DFB (nuDFB), contourlet, curvelet, shearlet and dual-tree wavelet. nuDFB is introduced in [2] based on multi-resolution analysis (MRA), where at each level of decomposition the square frequency domain is divided into a high frequency outer ring and a central low frequency domain. For nuDFB, the high frequency ring is primarily divided further into six equi-angular pairs of trapezoids and the central low frequency square is kept for division in the next level of decomposition, see Fig. 1. The nuDFB is solved by optimization which provides a non-unique near orthogonal or bi-orthogonal solution depending on the initialization. Contourlets [3] combine the Laplacian pyramid scheme

with DFB which has PR but with redundancy 4/3 inherited from the Laplacian pyramid. Shearlet [4, 5] and curvelet [6] systems construct a multi-resolution partition of the frequency domain by applying shear or rotation operators to a generator function in each level of frequency decomposition. Available shearlet and curvelet implementations have redundancy at least 4; moreover, the factor may grow with the number of directions in the decomposition level. Dual-tree wavelets [7] are linear combinations of 2D tensor wavelets (corresponding to multi-resolution systems) that constitute an approximate Hilbert transform pair, where the high frequency ring is divided into pairs of squares of different directional preference.

However, none of these multi-resolution schemes is PR, critically downsampled and regularized (localized in both time and frequency). In the framework of nuDFB ([2]), it is shown by Durand [8] that it's impossible to construct orthonormal filters localized in frequency without discontinuity in their frequency support, or equivalently regularized filters without aliasing. His construction of directional filters using compositions of 2-band filters associated to quincunx lattice, similar to that of uniform DFB in [2] and as pointed out in [2] the overall composed filters are not alias-free. Despite of Durand's disproof, it is not clear whether a regularized wavelet system exists if one slightly weaken the set of conditions.

To answer this question, we consider multi-resolution directional wavelets corresponding to the same partition of frequency domain as nuDFB and build a framework to analyze the equivalent conditions of PR for critically downsampled and more generally redundant schemes. In our previous work [9], we show that in MRA, PR is equivalent to an identity condition and shift-cancellation condition closely related to the frequency support of filters and their downsampling scheme. Based on these two conditions, we derive Durand's discontinuity result of orthonormal schemes and a relaxation of orthonormal schemes to frame with redundancy less than 2 that resolves the regularity limitation. Furthermore, we have an explicit approach to construct such regularized directional wavelet frames by smoothing the Fourier transform of the irregular directional wavelets. The main contribution of this paper is that we extend our previous work and show that the same irregularity in orthonormal schemes exists in bi-orthogonal schemes. Different from our previous approach in the orthonormal case, our analysis of bi-orthogonal schemes is based on a numerical algorithm introduced by Cohen et al in [10] for constructing compactly supported symmetric wavelet bases on hexagonal lattice. We extend and adapt this algorithm to our bi-orthogonal setting.

The paper is organized as follows, in section 2, we set up our framework of a dyadic MRA with dilated quincunx downsampling. In section 3, we review the irregularity of orthonormal schemes in [9]. In particular, we derive two conditions, *identity summation* and *shift cancellation*, equivalent to perfect reconstruction in this MRA with critical downsampling. These lead to the classification of *regular/singular* boundaries of the frequency partition and a *relaxed shift-cancellation* condition for low-redundancy MRA frame allows better regularity of the directional wavelets. In section 4, we show the irregularity for

bi-orthogonal schemes. We first review the wavelet construction algorithm in [10] which solves linear systems generated from regularity constraints. Next, we extend the algorithm to our framework and show that the resulting linear system doesn't have feasible solution satisfying all regularity constraints, especially continuity of Fourier transforms of wavelet filters. Finally, we conclude our results and discuss future work in section 7.

2 Framework Setup

We summarize 2D-MRA systems and the relation between frequency domain partition and sub-lattice of $\mathbb{Z}^2$ with critical downsampling following [9].

2.1 Notation

Throughout this paper, we use lower case normal font for function, upper case bold font for matrix, lower case bold font for vector and upper case normal font for frequency domain.

2.2 Multi-resolution analysis and sub-lattice sampling

In an MRA, given a scaling function $\phi \in L^2(\mathbb{R}^2)$, s.t. $\|\phi\|_2 = 1$, the base approximation space is defined as $V_0 = \overline{span\{\phi_{0,\boldsymbol{k}}\}_{\boldsymbol{k}\in\mathbb{Z}^2}}$, where $\phi_{0,\boldsymbol{k}} = \phi(\boldsymbol{x} - \boldsymbol{k})$. If $\langle \phi_{0,\boldsymbol{k}}, \phi_{0,\boldsymbol{k'}} \rangle = \delta_{\boldsymbol{k},\boldsymbol{k'}}$, then $\{\phi_{0,\boldsymbol{k}}\}$ is an orthonormal basis of V_0. In addition, ϕ is associated with a scaling matrix $\mathbf{D} \in \mathbb{Z}^{2\times 2}$, s.t. the dilated scaling function $\phi_1(\boldsymbol{x}) = |\mathbf{D}|^{-1/2}\phi(\mathbf{D}^{-1}\boldsymbol{x})$ is a linear combination of $\phi_{0,\boldsymbol{k}}$'s. Equivalently, $\exists\, m_0(\boldsymbol{\omega}) = m_0(\omega_1, \omega_2)$, $2\pi-$periodic in ω_1, ω_2, s.t. in the frequency domain

$$\widehat{\phi}(\mathbf{D}^T\boldsymbol{\omega}) = m_0(\boldsymbol{\omega})\widehat{\phi}(\boldsymbol{\omega}). \tag{1}$$

(1) implies that

$$\hat{\phi}(\boldsymbol{\omega}) = (2\pi)^{-1}\textstyle\prod_{k=1}^{\infty} m_0(\mathbf{D}^{-k}\boldsymbol{\omega}). \tag{2}$$

Let $\phi_{l,\boldsymbol{k}} = \phi(D^{-l}\boldsymbol{x} - \boldsymbol{k})$ and $V_l = \overline{span\{\phi_{l,\boldsymbol{k}}; \boldsymbol{k} \in \mathbb{Z}^2\}}$, $l \in \mathbb{Z}$ be the nested approximation spaces. Define W_l as the orthogonal complement of V_l with respect to V_{l-1} in MRA. Suppose there are J wavelet functions $\psi^j \in L^2(\mathbb{R}^2)$, $1 \le j \le J$, and $\mathbf{Q} \in \mathbb{Z}^{2\times 2}$, s.t.

$$W_1 = \bigcup_{j=1}^{J} W_1^j = \bigcup_{j=1}^{J} \overline{span\{\psi_{1,\boldsymbol{k}}^j; \boldsymbol{k} \in \mathbf{Q}\mathbb{Z}^2\}} = \bigcup_{j=1}^{J} \overline{span\{\psi^j(\mathbf{D}^{-1}\boldsymbol{x} - \boldsymbol{k}); \boldsymbol{k} \in \mathbf{Q}\mathbb{Z}^2\}},$$

an L-level multi-resolution system with base space V_0 is then spanned by

$$V_L \oplus \bigoplus_{l=1}^{L}\Big(\bigcup_{j=1}^{J} W_l^j\Big) = \{\phi_{L,\boldsymbol{k}}\,, \psi_{l,\boldsymbol{k'}}^j\,,\ 1 \le l \le L,\ \boldsymbol{k} \in \mathbb{Z}^2,\ \boldsymbol{k'} \in \mathbf{Q}\mathbb{Z}^2,\ 1 \le j \le J\}. \tag{3}$$

In particular, we set $\mathbf{D} = \mathbf{D_2} \doteq \left(\begin{smallmatrix} 2 & 0 \\ 0 & 2 \end{smallmatrix}\right)$ and $\mathbf{Q} := \left(\begin{smallmatrix} 1 & 1 \\ -1 & 1 \end{smallmatrix}\right)$. As $W_1 \subset V_0$, each rescaled wavelet $\psi^j(\mathbf{D}^{-1}\cdot)$ is also a linear combination of $\phi_{0,\boldsymbol{k}}$, so that $\exists\, m_j$

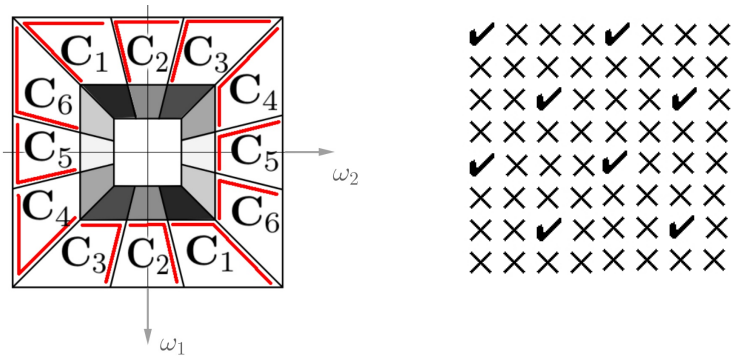

Figure 1: Left: partition of S_0 and boundary assignment of C_j, $j = 1, \cdots, 6$ (each C_j has boundaries indicated by red line segments), Right: dilated quincunx sub-lattice.

analogous to m_0 satisfying

$$\widehat{\psi^j}(\mathbf{D}^T\boldsymbol{\omega}) = m_j(\boldsymbol{\omega})\widehat{\phi}(\boldsymbol{\omega}), \qquad 1 \le j \le J. \tag{4}$$

In this specific construction of MRA, the corresponding subsampling matrix of $\phi_{1,\boldsymbol{k}}$ is $\mathbf{D}$ and that of $\psi^j_{1,\boldsymbol{k}}$ is $\mathbf{QD}$, the dilated quincunx subsample (see the right panel in Fig.1), as in [8].

2.3 Frequency domain partition and critical downsampling

Consider the canonical frequency square, $S_0 = [-\pi, \pi) \times [-\pi, \pi)$ associated with lattice $\mathcal{L} = \mathbb{Z}^2$. Consider a 1-level decomposition, (3) together with (1) and (4) implies that the union of the support of m_j, $0 \le j \le J$ covers S_0. Furthermore, $\exists\, C_j \subset supp(m_j), 0 \le j \le J$, such that they form a partition of S_0, and it is natural to take C_j as the main support of m_j. To build an orthonormal basis with good directional selectivity, we choose the partition of S_0 shown in the left of Fig.1, which is the same for Example B in [8] and the least redundant shearlet system. In this partition, S_0 is divided into a central square $C_0 = \left(\begin{smallmatrix} 2 & 0 \\ 0 & 2 \end{smallmatrix}\right)^{-1} S_0$ and a ring: the ring is further cut into six pairs of directional trapezoids C_j's by lines passing through the origin with slopes $\pm 1, \pm 3$ and $\pm\frac{1}{3}$. The central square C_0 can be further partitioned in the same way to obtain a two-level multi-resolution system, as shown in Fig.1.

Here $J = 6$ and $|\mathbf{D}|^{-1} + J|\mathbf{QD}|^{-1} = 1/4 + 6/(2 \cdot 4) = 1$, hence the corresponding MRA generated by (3) achieves critical downsampling([8]). In addition, let $\boldsymbol{\pi}_0 = (0,0), \boldsymbol{\pi}_1 = (\pi/2, \pi/2), \boldsymbol{\pi}_2 = (\pi, 0), \boldsymbol{\pi}_3 = (-\pi/2, \pi/2), \boldsymbol{\pi}_4 = (0, \pi), \boldsymbol{\pi}_5 = (\pi/2, -\pi/2), \boldsymbol{\pi}_6 = (\pi, \pi), \boldsymbol{\pi}_7 = (-\pi/2, -\pi/2)$, then each piece C_j together with its shifts form a tiling of S_0, i.e.

$$S_0 = \bigcup_{\boldsymbol{\pi} \in \Gamma_0} (C_j + \boldsymbol{\pi}) = \bigcup_{\boldsymbol{\pi} \in \Gamma_1} (C_0 + \boldsymbol{\pi}), \quad j = 1, \cdots, 6 \tag{5}$$

where $\Gamma_0 = \{\boldsymbol{\pi}_i,\, i = 0, 2, 4, 6\}$ and $\Gamma_1 = \{\boldsymbol{\pi}_i,\, i = 0, 1, \cdots, 7\}$. Alternatively, we say that $\{\, C_j,\, j = 0, \cdots, J \,\}$ is an *admissible* partition of S_0.

3 Orthonormal Bases

In this section, we discuss the conditions on $m-$ functions such that the corresponding MRA forms an orthonormal bases.

We begin with the two key conditions, i.e. *identity summation* and *shift cancellation*, on $m-$functions such that the system (3) is perfect reconstruction (PR) or equivalently a Parseval frame in MRA.

3.1 orthonormal conditions on $m-$functions

In MRA, (3) is PR if $\forall f \in L_2(\mathbb{R}^2)$,

$$\sum_k \langle f, \phi_{0,k}\rangle \phi_{0,k} = \sum_k \langle f, \phi_{1,k}\rangle \phi_{1,k} + \sum_j \sum_k \langle f, \psi^j_{1,k}\rangle \psi^j_{1,k}. \tag{6}$$

Using (1) and (4) together with the admissibility of the frequency partition (5), condition (6) on ϕ and ψ^j's yields:

Theorem 1. *The perfect reconstruction condition holds for* (3) *iff the following two conditions hold*

$$|m_0(\boldsymbol{\omega})|^2 + \sum_{j=1}^{6} |m_j(\boldsymbol{\omega})|^2 = 1 \tag{7}$$

$$\begin{cases} \sum_{j=0}^{6} m_j(\boldsymbol{\omega})\overline{m_j(\boldsymbol{\omega}+\boldsymbol{\pi})} = 0, & \boldsymbol{\pi} \in \Gamma_0 \setminus \{\mathbf{0}\} \\ \sum_{j=1}^{6} m_j(\boldsymbol{\omega})\overline{m_j(\boldsymbol{\omega}+\boldsymbol{\pi})} = 0, & \boldsymbol{\pi} \in \Gamma_1 \setminus \Gamma_0 \end{cases} \tag{8}$$

Theorem 1 is a corollary of Prop. 1 and Prop. 2 in [8]. We give an alternate proof in Appendix A. In Theorem 1, Eq. (7) is the *identity summation* condition, guaranteeing conservation of l_2 energy; Eq. (8) is the *shift cancellation* condition such that aliasing is canceled correctly in reconstruction from wavelet coefficients.

For (3) to be an orthonormal basis, $\{\phi_{\boldsymbol{k}}\}_{\boldsymbol{k}\in\mathbb{Z}^2}$ need to be an orthonormal basis, which is determined by m_0 in (2). In 1D MRA, Cohen's theorem in [11] provides a necessary and sufficient condition on m_0 such that (3) is an orthonormal basis. We generalized this theorem to 2D in [9].

Theorem 2. *Assume that m_0 is a trigonometric polynomial with $m_0(0) = 1$, and define $\hat{\phi}(\boldsymbol{\omega})$ as in* (2)*.*
If $\phi(\cdot - \boldsymbol{k}), \boldsymbol{k} \in \mathbb{Z}^2$ are orthonormal, then $\exists K$ containing a neighborhood of 0, s.t. $\forall \boldsymbol{\omega} \in S_0$, $\boldsymbol{\omega} + 2\pi\mathbf{n} \in K$ for some $\mathbf{n} \in \mathbb{Z}^2$, and $\inf_{k>0,\,\boldsymbol{\omega}\in K} |m_0(\mathbf{D_2}^{-k}\boldsymbol{\omega})| > 0$. Further, if $\sum_{\boldsymbol{\pi}\in\Gamma_0} |m_0(\boldsymbol{\omega}+\boldsymbol{\pi})|^2 = 1$, then the inverse is true.

3.2 m-function Design and Boundary Regularity

We begin with the Shannon-type wavelet construction. Let each m_j be an indicator function, $m_j = \mathbb{1}_{C_j}$, $0 \le j \le 6$, and we use the boundary assignment of C_j in Fig.1, then the identity summation follows from the partition, and the shift cancellation follows from (5). Applying Theorem 2 to m_0, we check that the

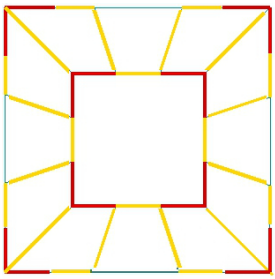

Figure 2: Boundary classification, singular (red) and regular (yellow)

Shannon-type wavelets generated from these $m-$functions form an orthonormal basis.

Such m_j's are not regularized due to the discontinuity on ∂C_j's, the boundaries of C_j's, hence the corresponding wavelets are not spatially localized. m_j's can be regularized by direct smoothing on ∂C_j's. However, as shown in Proposition 3 in [8], it is not possible to smooth all the boundaries with discontinuity if m_j's have to satisfy the perfect reconstruction condition. In [9], ∂C_j's are segmented into *singular* and *regular* pieces. On regular boundaries, pairs of $(m_j,\, m_{j'})$ that share the boundary can be smoothed in a coherent way such that all the constraints in Theorem 2 are satisfied. Yet, on those singular pieces, it is shown that m_j cannot be smoothed without violating the shift cancellation condition. Fig. 2 shows the boundary classification, where the corners of S_0 and C_0 are singular, hence m_0 and the diagonal $m-$ functions of an orthonormal bases are discontinuous there. A mechanism of constructing orthonormal bases by smoothing m_j on regular boundaries from indicator functions is provided in [9].

3.3 Extension to low-redundancy tight frame

The irregularity of orthonormal bases is overcome in the following low-redundancy tight frame construction,

$$\{\phi_{L,\boldsymbol{k}}\,, \psi^j_{l,\boldsymbol{k'}}\,,\ 1 \le l \le L,\ \boldsymbol{k},\, \boldsymbol{k'} \in \mathbb{Z}^2,\ 1 \le j \le J\}. \tag{9}$$

where all wavelet coefficients are sub-sampled on dyadic sub-lattice and the redundancy of any $L-$level MRA frame doesn't exceed $\frac{J/|D|}{1-1/|D|} = \frac{6/4}{1-1/4} = 2$. Similar to Theorem 2, we have

Theorem 3. *The perfect reconstruction condition holds for* (9) *iff the following both hold*

$$|m_0(\boldsymbol{\omega})|^2 + \textstyle\sum_{j=1}^{6} |m_j(\boldsymbol{\omega})|^2 = 1 \tag{10}$$

$$\textstyle\sum_{j=0}^{6}\, m_j(\boldsymbol{\omega})\overline{m_j(\boldsymbol{\omega}+\boldsymbol{\pi})} = 0, \quad \boldsymbol{\pi} \in \Gamma_0 \setminus \{\mathbf{0}\} \tag{11}$$

Theorem 3 can be proved analogously to Theorem 1, but with fewer shift cancellation constraints. Following the same analysis of boundary regularity as

previous, we show in [9] that all boundaries are regular and can be smoothed properly. We obtained directional wavelets with much better spatial and frequency localization than the one constructed by Durand in [8].

Heretofore, we have considered two directional wavelet MRA systems (3) and (9) such that the directional wavelets characterize 2D signals in six equi-angled directions. Furthermore, these wavelets are well localized in the frequency domain such that $supp(m_j)$ is convex and $\exists\, \epsilon\, s.t.$

$$\sup_{\boldsymbol{\omega}' \in supp(m_j)} \inf_{\boldsymbol{\omega} \in C_j} \|\boldsymbol{\omega}' - \boldsymbol{\omega}\| < \epsilon, \quad 0 \le j \le 6. \tag{12}$$

This desirable condition is hard to obtain by multi-directional filter bank assembly of several elementary filter banks.

In the next section, we analyze the more general case of directional bi-orthorgonal filters constructed with respect to the same frequency partition.

4 Bi-orthogonal Bases

In this section, we analyze bi-orthogonal bases in the following form of MRA,

$$\{\phi_{L,\boldsymbol{k}}, \widetilde{\phi}_{L,\boldsymbol{k}}, \psi^j_{l,\boldsymbol{k}'}, \widetilde{\psi}^j_{l,\boldsymbol{k}'},\ 1 \le l \le L,\ \boldsymbol{k} \in \mathbb{Z}^2,\ \boldsymbol{k}' \in \mathbf{Q}\mathbb{Z}^2,\ 1 \le j \le J\}, \tag{13}$$

where ϕ and ψ^j satisfy (1) and (4), as well as $\widetilde{\phi}$ and $\widetilde{\psi^j}$, respectively,

$$\widehat{\widetilde{\phi}}(\boldsymbol{D}^T\boldsymbol{\omega}) = \widetilde{m_0}(\boldsymbol{\omega})\widehat{\widetilde{\phi}}(\boldsymbol{\omega}), \quad \widehat{\widetilde{\psi^j}}(\boldsymbol{D}^T\boldsymbol{\omega}) = \widetilde{m_j}(\boldsymbol{\omega})\widehat{\widetilde{\phi}}(\boldsymbol{\omega}).$$

For such bi-orthogonal bases, we have the similar identity summation and shift cancellation condition to those in Theorem 1.

Theorem 4. *The perfect reconstruction iff the following two conditions hold*

$$m_0(\boldsymbol{\omega})\overline{\widetilde{m_0}}(\boldsymbol{\omega}) + \sum_{j=1}^{6} m_j(\boldsymbol{\omega})\overline{\widetilde{m_j}}(\boldsymbol{\omega}) = 1 \tag{14}$$

$$\begin{cases} \sum_{j=0}^{6} m_j(\boldsymbol{\omega})\overline{\widetilde{m_j}}(\boldsymbol{\omega}+\boldsymbol{\pi}) = 0, & \boldsymbol{\pi} \in \Gamma_0 \setminus \{\mathbf{0}\} \\ \sum_{j=1}^{6} m_j(\boldsymbol{\omega})\overline{\widetilde{m_j}}(\boldsymbol{\omega}+\boldsymbol{\pi}) = 0, & \boldsymbol{\pi} \in \Gamma_1 \setminus \Gamma_0 \end{cases} \tag{15}$$

The conditions (14) and (15) can be combined into a linear system as follows,

$$\begin{bmatrix} \overline{\widetilde{m_0}}(\boldsymbol{\omega}) & \overline{\widetilde{m_1}}(\boldsymbol{\omega}) & \dots & \overline{\widetilde{m_6}}(\boldsymbol{\omega}) \\ 0 & \overline{\widetilde{m_1}}(\boldsymbol{\omega}+\boldsymbol{\pi}_1) & \dots & \overline{\widetilde{m_6}}(\boldsymbol{\omega}+\boldsymbol{\pi}_1) \\ \overline{\widetilde{m_0}}(\boldsymbol{\omega}+\boldsymbol{\pi}_2) & \overline{\widetilde{m_1}}(\boldsymbol{\omega}+\boldsymbol{\pi}_2) & \dots & \overline{\widetilde{m_6}}(\boldsymbol{\omega}+\boldsymbol{\pi}_2) \\ \vdots & \vdots & \vdots & \vdots \\ 0 & \overline{\widetilde{m_1}}(\boldsymbol{\omega}+\boldsymbol{\pi}_7) & \dots & \overline{\widetilde{m_6}}(\boldsymbol{\omega}+\boldsymbol{\pi}_7) \end{bmatrix} \begin{bmatrix} m_0(\boldsymbol{\omega}) \\ m_1(\boldsymbol{\omega}) \\ m_2(\boldsymbol{\omega}) \\ \vdots \\ m_6(\boldsymbol{\omega}) \end{bmatrix} = \begin{bmatrix} 1 \\ 0 \\ 0 \\ \vdots \\ 0 \end{bmatrix} \tag{16}$$

In addition, we have the following analogue of Theorem 2.

Theorem 5. *Assume that $m_0, \widetilde{m_0}$ are trigonometric polynomials with $m_0(0) = \widetilde{m_0}(0) = 1$, which generate $\phi, \widetilde{\phi}$ respectively.*
If $\phi(\cdot - \boldsymbol{k}), \widetilde{\phi}(\cdot - \boldsymbol{k})$, $\boldsymbol{k} \in \mathbb{Z}^2$ are bi-orthogonal, then $\exists K$ containing a neighborhood of 0, s.t. $\forall \boldsymbol{\omega} \in S_0$, $\boldsymbol{\omega} + 2\pi\mathbf{n} \in K$ for some $\mathbf{n} \in \mathbb{Z}^2$, and $\inf_{k>0,\, \boldsymbol{\omega} \in K} |m_0(\mathbf{D_2}^{-k}\boldsymbol{\omega})| >$

0, $\inf_{k>0,\,\boldsymbol{\omega}\in K} |\widetilde{m_0}(\mathbf{D_2}^{-k}\boldsymbol{\omega})| > 0$. *Further, if* $\sum_{\boldsymbol{\pi}\in\Gamma_0} m_0(\boldsymbol{\omega}+\boldsymbol{\pi})\overline{\widetilde{m_0}}(\boldsymbol{\omega}+\boldsymbol{\pi}) = 1$, *then the inverse is true.*

By Theorem 5, m_0 and $\widetilde{m_0}$ need to satisfy the following identity constraint for the MRA (13) to be bi-orthogonal,

$$m_0\overline{\widetilde{m_0}}(\boldsymbol{\omega}) + m_0\overline{\widetilde{m_0}}(\boldsymbol{\omega}+\boldsymbol{\pi}_2) + m_0\overline{\widetilde{m_0}}(\boldsymbol{\omega}+\boldsymbol{\pi}_4) + m_0\overline{\widetilde{m_0}}(\boldsymbol{\omega}+\boldsymbol{\pi}_6) = 1. \quad (17)$$

In sum, the construction of a bi-orthogonal basis (13) is equivalent to find feasible solutions of (16) with constraint (17). To solve (16), we use the same approach in [10], which solves compactly supported symmetric bi-orthogonal filters on hexagon lattice. We next review the main scheme in [10] and extend it to our setup of directional wavelet filter.

4.1 Summary of Cohen et al's construction

We summerize the main setup and the approach in [10]. Consider a bi-orthogonal scheme consists of 3 high-pass filters m_1, m_2 and m_3 and a low-pass filter m_0 together with their bi-orthogonal duals $\widetilde{m_j}$, s.t. m_0 is $\frac{2\pi}{3}$-rotation invariant and m_1, m_2, m_3 are $\frac{2\pi}{3}$-rotation co-variant.

This bi-orthogonal scheme satisfies the following linear system (Lemma 2.2.2 in [10])

$$\begin{bmatrix} \overline{\widetilde{m_0}(\boldsymbol{\omega})} & \overline{\widetilde{m_1}(\boldsymbol{\omega})} & \overline{\widetilde{m_2}(\boldsymbol{\omega})} & \overline{\widetilde{m_3}(\boldsymbol{\omega})} \\ \overline{\widetilde{m_0}(\boldsymbol{\omega}+\boldsymbol{\nu}_1)} & \overline{\widetilde{m_1}(\boldsymbol{\omega}+\boldsymbol{\nu}_1)} & \overline{\widetilde{m_2}(\boldsymbol{\omega}+\boldsymbol{\nu}_1)} & \overline{\widetilde{m_3}(\boldsymbol{\omega}+\boldsymbol{\nu}_1)} \\ \vdots & \vdots & \vdots & \vdots \\ \overline{\widetilde{m_0}(\boldsymbol{\omega}+\boldsymbol{\nu}_3)} & \overline{\widetilde{m_1}(\boldsymbol{\omega}+\boldsymbol{\nu}_3)} & \overline{\widetilde{m_2}(\boldsymbol{\omega}+\boldsymbol{\nu}_3)} & \overline{\widetilde{m_3}(\boldsymbol{\omega}+\boldsymbol{\nu}_3)} \end{bmatrix} \begin{bmatrix} m_0(\boldsymbol{\omega}) \\ m_1(\boldsymbol{\omega}) \\ m_2(\boldsymbol{\omega}) \\ m_3(\boldsymbol{\omega}) \end{bmatrix} = \begin{bmatrix} 1 \\ 0 \\ 0 \\ 0 \end{bmatrix} \quad (18)$$

where $\boldsymbol{\nu}_1 = (\pi, 0), \boldsymbol{\nu}_2 = (0, \pi), \boldsymbol{\nu}_3 = (\pi, \pi)$. Let $\widetilde{\mathbf{M}}(\boldsymbol{\omega}) \in \mathbb{C}^{4\times 4}$ be the matrix with $\overline{\widetilde{m_j}(\boldsymbol{\omega})}$ entries and $\mathbf{m}(\boldsymbol{\omega}) \in \mathbb{C}^4$ be the vector with m_j entries in (18), then (18) can be written as $\widetilde{\mathbf{M}}\,\mathbf{m}(\boldsymbol{\omega}) = [1, 0, 0, 0]^\top$.

Given $\widetilde{m_1}(\boldsymbol{\omega})$, $\widetilde{m_2}(\boldsymbol{\omega})$, $\widetilde{m_3}(\boldsymbol{\omega})$ are determined by symmetry, and Lemma 2.2.2 in [10] shows that

$$\begin{aligned} m_0(\boldsymbol{\omega}) &= D^{-1} \begin{vmatrix} \overline{\widetilde{m_1}}(\boldsymbol{\omega}+\boldsymbol{\nu}_1) & \overline{\widetilde{m_2}}(\boldsymbol{\omega}+\boldsymbol{\nu}_1) & \overline{\widetilde{m_3}}(\boldsymbol{\omega}+\boldsymbol{\nu}_1) \\ \overline{\widetilde{m_1}}(\boldsymbol{\omega}+\boldsymbol{\nu}_2) & \overline{\widetilde{m_2}}(\boldsymbol{\omega}+\boldsymbol{\nu}_2) & \overline{\widetilde{m_3}}(\boldsymbol{\omega}+\boldsymbol{\nu}_2) \\ \overline{\widetilde{m_1}}(\boldsymbol{\omega}+\boldsymbol{\nu}_3) & \overline{\widetilde{m_2}}(\boldsymbol{\omega}+\boldsymbol{\nu}_3) & \overline{\widetilde{m_3}}(\boldsymbol{\omega}+\boldsymbol{\nu}_3) \end{vmatrix} \\ &= D^{-1}\det(\widetilde{\mathbf{M}}_{1,1}(\boldsymbol{\omega})), \end{aligned} \quad (19)$$

where $D \equiv \det(\widetilde{\mathbf{M}}) \in \mathbb{C}^* = \mathbb{C}\setminus\{0\}$. If $\widetilde{m_0}$ is solved, then m_1, m_2 and m_3 are obtained by solving the linear system (18). To get $\widetilde{m_0}(\boldsymbol{\omega})$, we solve

$$m_0\overline{\widetilde{m_0}}(\boldsymbol{\omega}) + m_0\overline{\widetilde{m_0}}(\boldsymbol{\omega}+\boldsymbol{\nu}_1) + m_0\overline{\widetilde{m_0}}(\boldsymbol{\omega}+\boldsymbol{\nu}_2) + m_0\overline{\widetilde{m_0}}(\boldsymbol{\omega}+\boldsymbol{\nu}_3) = 1 \quad (20)$$

from expanding $det(\widetilde{\mathbf{M}})$ with respect to the first column. According to Lemma 3.2.1 in [10] based on *Hilbert's Nullstellensatz*, (20) has a solution iff there does not exist $(z_1, z_2) \in (\mathbb{C}^*)^2$, $\mathbb{C}^* = \mathbb{C}\setminus\{0\}$ s.t. $(\pm z_1, \pm z_2)$ are all vanishing points of the z-transform of m_0.

4.1.1 Solving $\widetilde{m_0}(\boldsymbol{\omega})$

In general, there is no efficient algorithm to solve *Hilbert's Nullstellensatz*, and how (19) is solved exactly is not mentioned in [10].

We propose an optimization approach, where (19) is equivalent to a linear constraint and the objective function imposes regularity on $\widetilde{m_0}$. On a $2N \times 2N$ grid $\mathcal{G}$ of $S_0 = [-\pi, \pi) \times [-\pi, \pi)$, s.t. $\forall \boldsymbol{\omega}_j \in \mathcal{G}$, $\boldsymbol{\omega}_j + \boldsymbol{\nu}_1, \boldsymbol{\omega}_j + \boldsymbol{\nu}_2, \boldsymbol{\omega}_j + \boldsymbol{\nu}_3 \in \mathcal{G}$, (19) is reformulated as

$$\boldsymbol{A}\,\widetilde{\mathbf{m}}_{\mathbf{0}} = \mathbf{1}_{4N^2}, \tag{21}$$

$$\widetilde{\mathbf{m}}_{\mathbf{0}} = [\widetilde{m_0}(\boldsymbol{\omega}_i)]_{\,i=1,\ldots,4N^2} \quad \boldsymbol{A}_{i,j} = m_0(\boldsymbol{\omega}_j) \sum_{k=0}^{3} \delta(\boldsymbol{\omega}_j - \boldsymbol{\omega}_i - \boldsymbol{\nu}_k)$$

Because the set $\{\boldsymbol{\omega}, \boldsymbol{\omega} + \boldsymbol{\nu}_k, k = 1, 2, 3\}$ is invariant under the shift $\boldsymbol{\nu}_i$, $i = 1, 2, 3$, the rows of $\boldsymbol{A}$ corresponding to $\boldsymbol{\omega}$ and $\boldsymbol{\omega} + \boldsymbol{\nu}_i$ are identical and we only need to consider rows corresponds to $\boldsymbol{\omega} \in [-\pi, \pi) \times [-\pi, \pi)/\{\mathbf{0}, \boldsymbol{\nu}_i, i = 1, 2, 3\}$. Therefore, after removing the duplicate rows, $\boldsymbol{A} \in \mathbb{C}^{N^2 \times 4N^2}$ and (21) is underdeterminant.

We thus use (21) as a linear constraint in quadratic optimization to solve $\widetilde{\mathbf{m}}_{\mathbf{0}}$. Suppose that $\widetilde{m_0}(\boldsymbol{\omega})$ is smooth, then we build a differential operator $\boldsymbol{D}$ and solve the following minimization problem:

$$\min_{\widetilde{\mathbf{m}_0}} \|\boldsymbol{D}\widetilde{\mathbf{m}_0}\|^2, \quad s.t.\ \boldsymbol{A}\widetilde{\mathbf{m}_0} = \mathbf{1} \tag{22}$$

Or suppose $\widetilde{m_0}(\boldsymbol{\omega})$ decays away from the origin, then we build a diagonal weighting operator $\boldsymbol{W}$, and solve the following minimization problem:

$$\min_{\widetilde{\mathbf{m}_0}} \|\boldsymbol{W}\widetilde{\mathbf{m}_0}\|^2, \quad s.t.\ \boldsymbol{A}\widetilde{\mathbf{m}_0} = \mathbf{1} \tag{23}$$

Supplementary numerical results on solving $\widetilde{m_0}(\boldsymbol{\omega})$ by optimization are provided in Appendix B, where we test this optimization method on pre-designed biorthogonal filters m_0 and $\widetilde{m_0}$.

5 Adaptation to dilated quincunx scheme

Replace by an overview of this section

Following the same approach of Cohen et al, we focus on solving m_i's and $\widetilde{m_0}$ in (16) given pre-designed $\widetilde{m_i}(\boldsymbol{\omega})$, $i = 1, \cdots, 6$.

For simplicity, in the rest of this paper, we reuse notations for (18) to express (16) in the same form as $\widetilde{\mathbf{M}}\mathbf{m}(\boldsymbol{\omega}) = [1, 0, \cdots, 0]^T$, where $\widetilde{\mathbf{M}}(\boldsymbol{\omega}) \in \mathbb{C}^{8\times 7}$ and $\mathbf{m}(\boldsymbol{\omega}) \in \mathbb{C}^7$. In addition, for a matrix $\mathbf{A}$, we denote its sub-matrix containing all but the $k-$th column(row) as $\mathbf{A}[-k, :]$ ($\mathbf{A}[:, -k]$).In particular, we denote $\widetilde{\mathbf{M}}[-1, -1]$ as $\widetilde{\mathbf{M}}^{\square}$.

As in Section 4.1, we implicitly assume that $\widetilde{\mathbf{M}}(\boldsymbol{\omega})$ is full rank for any $\boldsymbol{\omega}$ so that (16) has unique solution $\boldsymbol{m}$ and Cramer's rule can be applied to compute m_0 with respect to a non-singular sub-matrix of $\widetilde{\mathbf{M}}$. That is, $\exists\, k_\omega \in \{2, \cdots, 8\}$

such that $\widetilde{\mathbf{M}}[-k_{\boldsymbol{\omega}},:]$ is non-singular[1]. Therefore,

$$m_0(\boldsymbol{\omega}) = \det(\widetilde{\mathbf{M}}^{\square}[-k_{\boldsymbol{\omega}},:])/\det(\widetilde{\mathbf{M}}[-k_{\boldsymbol{\omega}},:]). \tag{24}$$

Instead of requiring strong symmetries of $\widetilde{m_i}(\boldsymbol{\omega})$'s as in Section 4.1, we only ask for a minimum symmetry of $\widetilde{m_i}(\boldsymbol{\omega})$ such that $\widetilde{m_1}(\boldsymbol{\omega})$ and $\widetilde{m_6}(\boldsymbol{\omega})$ are symmetric with respect to the diagonal, and so are $\widetilde{m_3}(\boldsymbol{\omega})$ and $\widetilde{m_4}(\boldsymbol{\omega})$.

In the following subsections, we first show our main result that the pre-designed $\widetilde{m_i}$'s are discontinuous for (16) to be solvable. We then discuss how to design $\widetilde{m_i}$'s and solve the corresponding system (16).

5.1 Singularity of $\widetilde{\mathbf{M}}[-1,:]$ and discontinuity of $\widetilde{m_i}(\boldsymbol{\omega})$

Lemma 5.1. *If (16) is solvable, then $\widetilde{\mathbf{M}}[-1,:](\boldsymbol{\omega})$ is singular $\forall\boldsymbol{\omega}$.*

Proof. If (16) has a solution, then $\forall\boldsymbol{\omega}$, $[1,0,\cdots,0]^\top \in \mathbb{R}^8$ is a linear combination of the columns of $\widetilde{\mathbf{M}}$ hence the solution $\mathbf{m} \in Null(\widetilde{\mathbf{M}}[-1,:])$ and it is non-zero. This implies that $\widetilde{\mathbf{M}}[-1,:]$ is singular. □

Let $\widetilde{\mathbf{m}}^i(\boldsymbol{\omega}) = [\widetilde{m_1}(\boldsymbol{\omega}+\boldsymbol{\pi}_i)\ \cdots,\ \widetilde{m_6}(\boldsymbol{\omega}+\boldsymbol{\pi}_i)] \in \mathbb{C}^6$, $i = 0,\cdots,7$ be the rows of $\widetilde{\mathbf{M}}[:,-1]$, and define

$$d_{i,j}(\boldsymbol{\omega}) = \det([\widetilde{\mathbf{m}}^{k_1}(\boldsymbol{\omega})^\top,\cdots,\widetilde{\mathbf{m}}^{k_6}(\boldsymbol{\omega})^\top]),$$

where $\{k_l, l = 1,\cdots,6\} = \{0,\cdots,7\} \setminus \{i,j\}$.

Lemma 5.2. *$\widetilde{\mathbf{M}}[-1,:](\boldsymbol{\omega})$ is singular $\forall\boldsymbol{\omega}$ if and only if*

$$\mathfrak{D}(\omega)\begin{bmatrix}\widetilde{m_0}(\boldsymbol{\omega})\\ \widetilde{m_0}(\boldsymbol{\omega}+\boldsymbol{\pi}_2)\\ \widetilde{m_0}(\boldsymbol{\omega}+\boldsymbol{\pi}_4)\\ \widetilde{m_0}(\boldsymbol{\omega}+\boldsymbol{\pi}_6)\end{bmatrix} \doteq \begin{bmatrix}0 & d_{0,2} & d_{0,4} & d_{0,6}\\ -d_{0,2} & 0 & d_{2,4} & d_{2,6}\\ -d_{0,4} & -d_{2,4} & 0 & d_{4,6}\\ -d_{0,6} & -d_{2,6} & -d_{4,6} & 0\end{bmatrix}\begin{bmatrix}\widetilde{m_0}(\boldsymbol{\omega})\\ \widetilde{m_0}(\boldsymbol{\omega}+\boldsymbol{\pi}_2)\\ \widetilde{m_0}(\boldsymbol{\omega}+\boldsymbol{\pi}_4)\\ \widetilde{m_0}(\boldsymbol{\omega}+\boldsymbol{\pi}_6)\end{bmatrix} = \begin{bmatrix}0\\0\\0\\0\end{bmatrix}. \tag{25}$$

Proof. The singularity condition on $\widetilde{\mathbf{M}}[-1,:](\boldsymbol{\omega})$ can be rewritten as follows,

$$\begin{aligned}0 &= \det(\widetilde{\mathbf{M}}[-1,:])\\ &= \widetilde{m_0}(\boldsymbol{\omega}+\boldsymbol{\pi}_2)\cdot\det(\widetilde{\mathbf{M}}^{\square}[-2,:])\\ &\quad + \widetilde{m_0}(\boldsymbol{\omega}+\boldsymbol{\pi}_4)\cdot\det(\widetilde{\mathbf{M}}^{\square}[-4,:]) + \widetilde{m_0}(\boldsymbol{\omega}+\boldsymbol{\pi}_6)\cdot\det(\widetilde{\mathbf{M}}^{\square}[-6,:])\\ &= 0\cdot\widetilde{m_0}(\boldsymbol{\omega}) + d_{0,2}\cdot\widetilde{m_0}(\boldsymbol{\omega}+\boldsymbol{\pi}_2)\\ &\quad + d_{0,4}\cdot\widetilde{m_0}(\boldsymbol{\omega}+\boldsymbol{\pi}_4) + d_{0,6}\cdot\widetilde{m_0}(\boldsymbol{\omega}+\boldsymbol{\pi}_6)\end{aligned} \tag{26}$$

This is the first equation in the linear system (25). Substitute $\boldsymbol{\omega}$ by $\boldsymbol{\omega}+\boldsymbol{\pi_2}$ in (26) and use the $2\pi-$periodicity of $\boldsymbol{\omega}$, we have the singularity condition on $\widetilde{\mathbf{M}}[-1,:](\boldsymbol{\omega}+\boldsymbol{\pi_2})$ as follows

$$-d_{0,2}(\boldsymbol{\omega})\cdot\widetilde{m_0}(\boldsymbol{\omega}) + d_{2,4}(\boldsymbol{\omega})\cdot\widetilde{m_0}(\boldsymbol{\omega}+\boldsymbol{\pi}_4) + d_{2,6}(\boldsymbol{\omega})\cdot\widetilde{m_0}(\boldsymbol{\omega}+\boldsymbol{\pi}_6) = 0,$$

which is the second linear equation in (25). Similarly, the third and fourth equations can be obtained by rewriting the singularity condition at $\boldsymbol{\omega}+\boldsymbol{\pi}_4$ and $\boldsymbol{\omega}+\boldsymbol{\pi}_6$ in the coordinate of $\boldsymbol{\omega}$. □

[1]Lemma 5.1 shows that $k_\omega \neq 1$

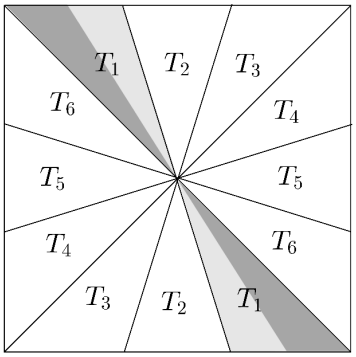

Figure 3: Partition of frequency square in six directions, where the essential support of $\widetilde{m_i}(\boldsymbol{\omega})$ is contained in each pair of triangles T_i. The pair of dark grey triangles is T_1^- and the light grey pair is T_1^+.

The identity constraint (17) on m_0 and the singularity condition (25) together imply the following proposition,

Proposition 5.3. *Given $\widetilde{m_i}, i = 1, \cdots, 6$, (16) has no solution for $\widetilde{m_0}$, if $\exists\, \omega$, s.t.$[m_0(\omega), m_0(\omega+\pi_2), m_0(\omega+\pi_4), m_0(\omega+\pi_6)]$ is a linear combination of the conjugate of the rows of $\mathfrak{D}(\omega)$.*

Definition. The *essential support* Ω_i of a function $\widetilde{m_i}$ is the set $\{\boldsymbol{\omega} : |\widetilde{m_i}(\boldsymbol{\omega})| > |\widetilde{m_j}(\boldsymbol{\omega})|, \forall j \neq i\}$.

Let T_i be pairs of triangles shown in Figure 3, such that $C_i \subset T_i$, $i = 1, \cdots, 6$. Consider its decomposition, $T_i = T_i^- \bigcup T_i^+$, where T_i^-, T_i^+ are halves of T_i adjacent to T_{i-1} and T_{i+1} respectively.

Definition. $\widetilde{m_i}$ *concentrates* within cone T_i if

(i) $\Omega_i \subset T_i$;

(ii) $\mathrm{supp}(\widetilde{m_i}) \subset T_{i-1}^+ \bigcup T_i \bigcup T_{i+1}^-$ and $\int_\Omega |\widetilde{m_i}| > \int_{\Omega'} |\widetilde{m_i}|, \forall\, \Omega \subset T_i \bigcap \mathrm{supp}(\widetilde{m_i})$, where $\Omega' \subset T_{i-1}^+ \bigcup T_{i+1}^-$ is symmetric to Ω with respect to the boundary of T_i.

Given $\widetilde{m_i}(\boldsymbol{\omega})$ that concentrates in T_i, we study the feasibility condition in Proposition 5.3 specifically on the domain $S_\rho = \{(\omega_1, \omega_2) |\ \|\omega\| < \rho, \omega_1 < 0, \omega_2 < 0\}$, see Figure 4.

Lemma 5.4. *$\exists\, \rho > 0$ s.t. $\forall \omega \in S_\rho$, $rank(\widetilde{\mathbf{m}}^1, \widetilde{\mathbf{m}}^7) = 1$.*

Proof. When ρ is small enough, due to the concentration property, $\widetilde{m_i}(\boldsymbol{\omega})$ is zero on all but a few sets $S_\rho + \boldsymbol{\pi}_j$ (see Fig.4 for reference of S_ρ and its shifts),

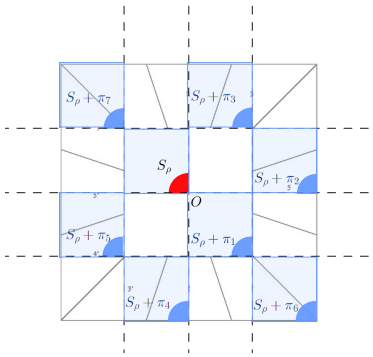

Figure 4: S_ρ and its shifts

thus $\widetilde{\mathbf{m}}^i(\boldsymbol{\omega})$ is sparse on S_ρ and $\widetilde{\mathbf{M}}[-1,:]$ takes the following form

$$\widetilde{\mathbf{M}}[-1,:](\boldsymbol{\omega}) = \begin{bmatrix} \widetilde{\mathbf{m}}^0 \\ \widetilde{\mathbf{m}}^1 \\ \widetilde{\mathbf{m}}^2 \\ \widetilde{\mathbf{m}}^3 \\ \widetilde{\mathbf{m}}^4 \\ \widetilde{\mathbf{m}}^5 \\ \widetilde{\mathbf{m}}^6 \\ \widetilde{\mathbf{m}}^7 \end{bmatrix} = \begin{bmatrix} 0 & 0 & 0 & 0 & 0 & 0 \\ * & 0 & 0 & 0 & 0 & * \\ 0 & * & * & 0 & 0 & 0 \\ 0 & 0 & * & * & 0 & 0 \\ 0 & 0 & 0 & * & * & 0 \\ 0 & 0 & * & * & 0 & 0 \\ * & 0 & 0 & 0 & 0 & * \\ * & 0 & 0 & 0 & 0 & * \end{bmatrix} \tag{27}$$

where $*$s denote possible non-zero entries. We make the following observation of $\widetilde{\mathbf{m}}^i$:

(i) $\widetilde{\mathbf{m}}^0$ is a zero vector

(ii) $\widetilde{\mathbf{m}}^2$ and $\widetilde{\mathbf{m}}^4$ are linearly independent of each other and the rest of $\widetilde{\mathbf{m}}^i$

(iii) $span\{\widetilde{\mathbf{m}}^1, \widetilde{\mathbf{m}}^6, \widetilde{\mathbf{m}}^7\} \perp span\{\widetilde{\mathbf{m}}^3, \widetilde{\mathbf{m}}^5\}$ and $rank(\widetilde{\mathbf{m}}^1, \widetilde{\mathbf{m}}^6, \widetilde{\mathbf{m}}^7) \leq 2$, $rank(\widetilde{\mathbf{m}}^3, \widetilde{\mathbf{m}}^5) \leq 2$

Since S_ρ is in the low frequency domain, $m_0(\boldsymbol{\omega}) \neq 0$. (24) then implies that $\widetilde{\mathbf{M}}^\square$ is full rank, or equivantly, $rank(\widetilde{\mathbf{M}}[-1,:]) = 6$. It follows from (ii) and (iii) that $rank(\widetilde{\mathbf{m}}^1, \widetilde{\mathbf{m}}^6, \widetilde{\mathbf{m}}^7) = 2$ and $rank(\widetilde{\mathbf{m}}^3, \widetilde{\mathbf{m}}^5) = 2$.
On the other hand, (ii) implies that

$$rank(\widetilde{\mathbf{M}}^\square(\boldsymbol{\omega} + \boldsymbol{\pi}_2)) = rank(\widetilde{\mathbf{m}}^4, \widetilde{\mathbf{m}}^6, \widetilde{\mathbf{m}}^1, \widetilde{\mathbf{m}}^3, \widetilde{\mathbf{m}}^5, \widetilde{\mathbf{m}}^7) \leq 5$$

and likewise

$$rank(\widetilde{\mathbf{M}}^\square(\boldsymbol{\omega} + \boldsymbol{\pi}_4)) = rank(\widetilde{\mathbf{m}}^2, \widetilde{\mathbf{m}}^6, \widetilde{\mathbf{m}}^1, \widetilde{\mathbf{m}}^3, \widetilde{\mathbf{m}}^5, \widetilde{\mathbf{m}}^7) \leq 5.$$

Therefore, $\det(\widetilde{\mathbf{M}}^\square(\boldsymbol{\omega} + \boldsymbol{\pi}_2)) = \det(\widetilde{\mathbf{M}}^\square(\boldsymbol{\omega} + \boldsymbol{\pi}_4)) = 0$ and (24) implies $m_0(\boldsymbol{\omega} + \boldsymbol{\pi}_2) = m_0(\boldsymbol{\omega} + \boldsymbol{\pi}_4) = 0$.
If $\widetilde{\mathbf{m}}^1$ and $\widetilde{\mathbf{m}}^7$ are linearly independent, then $rank(\widetilde{\mathbf{m}}^2, \widetilde{\mathbf{m}}^4, \widetilde{\mathbf{m}}^1, \widetilde{\mathbf{m}}^3, \widetilde{\mathbf{m}}^5, \widetilde{\mathbf{m}}^7) = 6$, hence $m_0(\boldsymbol{\omega} + \boldsymbol{\pi}_6) \neq 0$. Therefore, $[m_0(\boldsymbol{\omega}), m_0(\boldsymbol{\omega} + \boldsymbol{\pi}_2), m_0(\boldsymbol{\omega} + \boldsymbol{\pi}_4), m_0(\boldsymbol{\omega} + \boldsymbol{\pi}_6)] = [*, 0, 0, *]$. In addition, $d_{i,j} = 0$, $\forall (i,j)$ except $(0,6)$, so

$$\mathfrak{D}(\boldsymbol{\omega}) = [d_{0,6}, 0, 0, 0]^\top [0, 0, 0, 1] + [0, 0, 0, d_{0,6}]^\top [-1, 0, 0, 0].$$

By Proposition 5.3, the linear system (16) has no solution $\widetilde{m_0}$ and this proofs the lemma. □

Lemma 5.5. *If $\widetilde{m_1}(\boldsymbol{\omega})(\widetilde{m_6}(\boldsymbol{\omega}))$ concentrates in $T_1(T_6)$, then $|\widetilde{m_6}(\boldsymbol{\omega})| > |\widetilde{m_1}(\boldsymbol{\omega})|$ a.e. on $T_6 \bigcap supp(\widetilde{m_6})$ ($|\widetilde{m_1}(\boldsymbol{\omega})| > |\widetilde{m_6}(\boldsymbol{\omega})|$ a.e. on $T_1 \bigcap supp(\widetilde{m_1})$).*

Proof Let $B_6 = \{\boldsymbol{\omega} : |\widetilde{m_6}(\boldsymbol{\omega})| \leq |\widetilde{m_1}(\boldsymbol{\omega})|\} \bigcap T_6 \bigcap supp(\widetilde{m_1})$ and B_1 be its mirror set with respect to $\omega_1 = \omega_2$ and suppose $|B_6| > 0$, then $\int_{B_6} |\widetilde{m_6}(\boldsymbol{\omega})| \leq \int_{B_6} |\widetilde{m_1}(\boldsymbol{\omega})|$. Since $\widetilde{m_1}(\boldsymbol{\omega})$ concentrates in T_1, we know $\int_{B_1} |\widetilde{m_1}(\boldsymbol{\omega})| > \int_{B_6} |\widetilde{m_1}(\boldsymbol{\omega})|$. On the other hand, due to the symmetry of $\widetilde{m_1}(\boldsymbol{\omega}), \widetilde{m_6}(\boldsymbol{\omega})$ and B_1, B_6, $\int_{B_1} |\widetilde{m_1}(\boldsymbol{\omega})| = \int_{B_6} |\widetilde{m_6}(\boldsymbol{\omega})|$, hence $\int_{B_6} |\widetilde{m_1}(\boldsymbol{\omega})| \geq \int_{B_6} |\widetilde{m_6}(\boldsymbol{\omega})| = \int_{B_1} |\widetilde{m_1}(\boldsymbol{\omega})|$ which results in contradiction. □

Proposition 5.6. *If m_1 (m_6) concentrates within T_1 (T_6), then $\widetilde{m_1}(\boldsymbol{\omega}) = \widetilde{m_6}(\boldsymbol{\omega}) = 0$, a.e. $\boldsymbol{\omega} \in S_\rho + \boldsymbol{\pi}_1$.*

Proof. Consider frequency domain $S'_\rho = S_\rho \bigcap \{\omega_1 < \omega_2\}$. By Lemma 5.4, $\exists\, \alpha_{\boldsymbol{\omega}} \in \mathbb{C}, s.t. \widetilde{\mathbf{m}}^1(\boldsymbol{\omega}) = \alpha_{\boldsymbol{\omega}} \widetilde{\mathbf{m}}^7(\boldsymbol{\omega}), \forall\, \boldsymbol{\omega} \in S'_\rho$, i.e. $\widetilde{m_1}(\boldsymbol{\omega} + \boldsymbol{\pi}_1) = \alpha_{\boldsymbol{\omega}} \cdot \widetilde{m_1}(\boldsymbol{\omega} + \boldsymbol{\pi}_7)$ and $\widetilde{m_6}(\boldsymbol{\omega} + \boldsymbol{\pi}_1) = \alpha_{\boldsymbol{\omega}} \cdot \widetilde{m_6}(\boldsymbol{\omega} + \boldsymbol{\pi}_7)$. On the other hand, Lemma 5.5 implies that $|\widetilde{m_1}(\boldsymbol{\omega} + \boldsymbol{\pi}_7)| \geq |\widetilde{m_6}(\boldsymbol{\omega} + \boldsymbol{\pi}_7)|$, hence $|\widetilde{m_1}(\boldsymbol{\omega} + \boldsymbol{\pi}_1)| \geq |\widetilde{m_6}(\boldsymbol{\omega} + \boldsymbol{\pi}_1)|$. Let $\Omega'_6 := (S_\rho + \pi_1) \bigcap T_6$, then $\int_{\Omega'_6} |\widetilde{m_1}(\boldsymbol{\omega})| \geq \int_{\Omega'_6} |\widetilde{m_6}(\boldsymbol{\omega})|$, which will contradict Lemma 5.5 unless $|\Omega'_6 \bigcap \mathrm{supp}(\widetilde{m_6})| = 0$, or equivalently $\alpha_{\boldsymbol{\omega}} = 0$ and so $\widetilde{m_6}(\boldsymbol{\omega}) = \widetilde{m_1}(\boldsymbol{\omega}) = 0$, *a.e.* on Ω'_6. By symmetry, $\widetilde{m_6}(\boldsymbol{\omega}) = \widetilde{m_1}(\boldsymbol{\omega}) = 0$, *a.e.* on $(S_\rho + \boldsymbol{\pi}_1) \backslash \Omega'_6$ as well. □

Proposition 5.7. *$\widetilde{m_1}(\boldsymbol{\omega}), \widetilde{m_6}(\boldsymbol{\omega})$ are not continuous at both $(\frac{\pi}{2}, \frac{\pi}{2})$ and $(-\frac{\pi}{2}, -\frac{\pi}{2})$.*

Proof If $\widetilde{m_1}(\boldsymbol{\omega})$ is continuous at $(\frac{\pi}{2}, \frac{\pi}{2})$, then $\widetilde{m_1}(\frac{\pi}{2}, \frac{\pi}{2}) = \lim_{\alpha \to 1^-} \widetilde{m_1}(\boldsymbol{\omega}(\alpha)) = 0$, where $\{\boldsymbol{\omega}(\alpha), 0 \leq \alpha < 1\} \subset S_\rho + \boldsymbol{\pi}_1$ and $\boldsymbol{\omega}(1) = (\frac{\pi}{2}, \frac{\pi}{2})$. Similarly, we have $\widetilde{m_6}(\frac{\pi}{2}, \frac{\pi}{2}) = 0$. The continuity at $(-\frac{\pi}{2}, -\frac{\pi}{2})$ implies $\widetilde{m_1}(-\frac{\pi}{2}, -\frac{\pi}{2}) = \widetilde{m_6}(-\frac{\pi}{2}, -\frac{\pi}{2}) = 0$. Therefore $\widetilde{\mathbf{m}}^1(0) = \widetilde{\mathbf{m}}^7(0) = \mathbf{0}$ which results in contradiction with Lemma 5.4. □

The following theorem summarizes our main result.

Theorem 5.8. *If $\widetilde{m_i}(\boldsymbol{\omega})$ concentrates in T_i and $\widetilde{m_1}(\boldsymbol{\omega}), \widetilde{m_6}(\boldsymbol{\omega})$ are symmetric to each other, then* (16) *doesn't have feasible solution given continuous $\widetilde{m_1}(\boldsymbol{\omega})$ and $\widetilde{m_6}(\boldsymbol{\omega})$.*

5.2 Design of input $\widetilde{m_i}(\boldsymbol{\omega})$

Following the orthonormal construction in [9], we consider $\widetilde{m_1}(\boldsymbol{\omega}), \cdots, \widetilde{m_6}(\boldsymbol{\omega})$ in the form

$$\widetilde{m_k}(\boldsymbol{\omega}) = e^{-i\boldsymbol{\eta}_k^\top \boldsymbol{\omega}} |\widetilde{m_k}(\boldsymbol{\omega})|, \tag{28}$$

and $|\widetilde{m_k}(\boldsymbol{\omega})|$ have certain symmetry. We want to design the phase $\boldsymbol{\eta}_k$ such that $m_0(\boldsymbol{\omega}) > 0$, $\forall \omega \in S_1$. This is the same as requiring $\widetilde{\mathbf{M}}^\square$ to be full rank. We first show the necessary conditions on phases $\boldsymbol{\eta}$ of the full rank requirement on $\widetilde{\mathbf{M}}^\square$.

Lemma 5.9. *If* $\exists\, \boldsymbol{\omega} \in D_1 := \{\omega_x = \omega_y, \omega_x \in (-\frac{\pi}{2}, 0)\}$, *s.t.* $m_0(\boldsymbol{\omega}) > 0$, *then* $(\boldsymbol{\eta}_1 - \boldsymbol{\eta}_6)^\top (\boldsymbol{\pi}_6 - \boldsymbol{\pi}_7) \neq 0 (mod\, 2\pi)$.

Proof If $m_0(\boldsymbol{\omega}) > 0, \boldsymbol{\omega} \in D_1$ then $\widetilde{\mathbf{M}}^{\square}$ is full rank, hence its columns are linearly independent. Due to symmetry, $|\widetilde{m_1}(\boldsymbol{\omega})| = |\widetilde{m_6}(\boldsymbol{\omega})|$ on $\{\omega_x = \omega_y\}$. Let $A = |\widetilde{m_1}(\boldsymbol{\omega} + \boldsymbol{\pi}_1)| = |\widetilde{m_6}(\boldsymbol{\omega} + \boldsymbol{\pi}_1)|$ and $B = |\widetilde{m_1}(\boldsymbol{\omega} + \boldsymbol{\pi}_6)| = |\widetilde{m_6}(\boldsymbol{\omega} + \boldsymbol{\pi}_6)|$, then the first and the last columns of $\widetilde{\mathbf{M}}^{\square}$ are

$$\widetilde{\mathbf{M}}^{\square}[:,1] = \begin{bmatrix} 0 \\ \vdots \\ 0 \\ Ae^{i\boldsymbol{\eta}_1^\top(\boldsymbol{\omega}+\boldsymbol{\pi}_6)} \\ Be^{i\boldsymbol{\eta}_1^\top(\boldsymbol{\omega}+\boldsymbol{\pi}_7)} \end{bmatrix} \quad \text{and} \quad \widetilde{\mathbf{M}}^{\square}[:,6] = \begin{bmatrix} 0 \\ \vdots \\ 0 \\ Ae^{i\boldsymbol{\eta}_6^\top(\boldsymbol{\omega}+\boldsymbol{\pi}_6)} \\ Be^{i\boldsymbol{\eta}_6^\top(\boldsymbol{\omega}+\boldsymbol{\pi}_7)} \end{bmatrix}.$$

Therefore, $\widetilde{\mathbf{M}}^{\square}[:,1]$ and $\widetilde{\mathbf{M}}^{\square}[:,6]$ are linearly independent implies that $e^{i(\boldsymbol{\eta}_1-\boldsymbol{\eta}_6)^\top(\boldsymbol{\omega}+\boldsymbol{\pi}_6)} \neq e^{i(\boldsymbol{\eta}_1-\boldsymbol{\eta}_6)^\top(\boldsymbol{\omega}+\boldsymbol{\pi}_7)}$ or equivalently $(\boldsymbol{\eta}_1 - \boldsymbol{\eta}_6)^\top (\boldsymbol{\pi}_6 - \boldsymbol{\pi}_7) \neq 0 (\mathrm{mod} 2\pi)$. □

Similarly, if $\exists\, \boldsymbol{\omega} \in \{\omega_y = \omega_x, \omega_x \in (0, \frac{\pi}{2})\}$, *s.t.* $m_0(\boldsymbol{\omega}) > 0$, then $(\boldsymbol{\eta}_1 - \boldsymbol{\eta}_6)^\top (\boldsymbol{\pi}_6 - \boldsymbol{\pi}_1) \neq 0 (\mathrm{mod}\, 2\pi)$. These two conditions are equivalent to

$$(\boldsymbol{\eta}_1 - \boldsymbol{\eta}_6)^\top (\pi/2, \pi/2) \neq 0 (\mathrm{mod}\, 2\pi) \qquad \textbf{(c1.1)}$$

given that $\boldsymbol{\eta}_1$ and $\boldsymbol{\eta}_6$ are integer phases. A stronger condition is to require $\widetilde{\mathbf{M}}^{\square}[:,1]$ and $\widetilde{\mathbf{M}}^{\square}[:,6]$ be orthogonal, which is equivalent to

$$(\boldsymbol{\eta}_1 - \boldsymbol{\eta}_6)^\top (\pi/2, \pi/2) = \pi\, (\mathrm{mod}\, 2\pi). \qquad \textbf{(c2.1)}$$

Considering the other diagonal segment $\{\omega_y = -\omega_x, |\omega_x| < \frac{\pi}{2}\}$, we have

$$(\boldsymbol{\eta}_3 - \boldsymbol{\eta}_4)^\top (-\pi/2, \pi/2) \neq 0 (\mathrm{mod}\, 2\pi) \qquad \textbf{(c1.2)}$$

from the full rank condition and

$$(\boldsymbol{\eta}_3 - \boldsymbol{\eta}_4)^\top (-\pi/2, \pi/2) = \pi (\mathrm{mod},\, 2\pi) \qquad \textbf{(c2.2)}$$

from the stronger orthogonal condition. *Remark* If $|\widetilde{m_1}(\boldsymbol{\omega})| = |\widetilde{m_2}(\boldsymbol{\omega})|$ on $\{\omega_y = 3\omega_x, |\omega_x| > \frac{\pi}{2}\}$ and $m_0(\boldsymbol{\omega}) > 0$ on $\{\omega_y = 3\omega_x \pm \pi, |\omega_y| < \frac{\pi}{2}\}$, then the same conditions (**c1**) and (**c2**) can be derived from full rank and orthogonal conditions respectively for tuples $(\boldsymbol{\eta}_1, \boldsymbol{\eta}_2, (-\pi/2, \pi/2))$, $(\boldsymbol{\eta}_2, \boldsymbol{\eta}_3, (\pi/2, \pi/2))$, $(\boldsymbol{\eta}_4, \boldsymbol{\eta}_5, (\pi/2, \pi/2))$ and $(\boldsymbol{\eta}_5, \boldsymbol{\eta}_6, (-\pi/2, \pi/2))$.

Next, we investigate $\widetilde{\mathbf{M}}^{\square}$ at the origin, where the two diagonals meet.

Proposition 5.10. *If* $m_0(0) > 0$, *then* $\boldsymbol{\pi}_1^\top (\boldsymbol{\eta}_1 - \boldsymbol{\eta}_6) \neq \pi (mod\, 2\pi)$ *or* $\boldsymbol{\pi}_3^\top (\boldsymbol{\eta}_3 - \boldsymbol{\eta}_4) \neq \pi (mod\, 2\pi)$.

Proof $\widetilde{\mathbf{M}}^{\square}(0)$ takes the following form

$$\begin{bmatrix} * & 0 & 0 & 0 & 0 & * \\ 0 & * & 0 & 0 & 0 & 0 \\ 0 & 0 & * & * & 0 & 0 \\ 0 & 0 & 0 & 0 & * & 0 \\ 0 & 0 & * & * & 0 & 0 \\ * & 0 & * & * & 0 & * \\ * & 0 & 0 & 0 & 0 & * \end{bmatrix}$$

The second and the fifth columns of $\widetilde{\mathbf{M}}^{\square}$ have single non-zero entry, $\widetilde{m_2}(\boldsymbol{\pi}_2)$ and $\widetilde{m_5}(\boldsymbol{\pi}_4)$ respectively, and are orthogonal to all the rest columns, hence the full-rank constraint of $\widetilde{\mathbf{M}}^{\square}$ is reduced to the full-rank constraint on its sub-matrix (with permutation of rows and columns)

$$\overline{\mathrm{B}} := \overline{\widetilde{\mathbf{M}}^{\square}}[-2,-4,:] = \begin{bmatrix} \widetilde{m_1}(\boldsymbol{\pi}_6) & \widetilde{m_6}(\boldsymbol{\pi}_6) & \widetilde{m_3}(\boldsymbol{\pi}_6) & \widetilde{m_4}(\boldsymbol{\pi}_6) \\ \widetilde{m_1}(\boldsymbol{\pi}_1) & \widetilde{m_6}(\boldsymbol{\pi}_1) & 0 & 0 \\ \widetilde{m_1}(\boldsymbol{\pi}_7) & \widetilde{m_6}(\boldsymbol{\pi}_7) & 0 & 0 \\ 0 & 0 & \widetilde{m_3}(\boldsymbol{\pi}_3) & \widetilde{m_4}(\boldsymbol{\pi}_3) \\ 0 & 0 & \widetilde{m_3}(\boldsymbol{\pi}_5) & \widetilde{m_4}(\boldsymbol{\pi}_5) \end{bmatrix}$$

Without loss of generality, let $|\widetilde{m_1}(\boldsymbol{\pi}_1)| = |\widetilde{m_1}(\boldsymbol{\pi}_7)| = |\widetilde{m_6}(\boldsymbol{\pi}_1)| = |\widetilde{m_6}(\boldsymbol{\pi}_7)| = |\widetilde{m_3}(\boldsymbol{\pi}_3)| = |\widetilde{m_3}(\boldsymbol{\pi}_5)| = |\widetilde{m_4}(\boldsymbol{\pi}_3)| = |\widetilde{m_4}(\boldsymbol{\pi}_5)| = a$ and $|\widetilde{m_1}(\boldsymbol{\pi}_6)| = |\widetilde{m_6}(\boldsymbol{\pi}_6)| = |\widetilde{m_3}(\boldsymbol{\pi}_6)| = |\widetilde{m_4}(\boldsymbol{\pi}_6)| = b$. Rewrite $\overline{\mathrm{B}}$ as follows,

$$\overline{\mathrm{B}} = \begin{bmatrix} be^{-i\boldsymbol{\pi}_6^\top \boldsymbol{\eta}_1} & be^{-i\boldsymbol{\pi}_6^\top \boldsymbol{\eta}_6} & be^{-i\boldsymbol{\pi}_6^\top \boldsymbol{\eta}_3} & be^{-i\boldsymbol{\pi}_6^\top \boldsymbol{\eta}_4} \\ ae^{-i\boldsymbol{\pi}_1^\top \boldsymbol{\eta}_1} & ae^{-i\boldsymbol{\pi}_1^\top \boldsymbol{\eta}_6} & 0 & 0 \\ ae^{i\boldsymbol{\pi}_1^\top \boldsymbol{\eta}_1} & ae^{i\boldsymbol{\pi}_1^\top \boldsymbol{\eta}_6} & 0 & 0 \\ 0 & 0 & ae^{-i\boldsymbol{\pi}_3^\top \boldsymbol{\eta}_3} & ae^{-i\boldsymbol{\pi}_3^\top \boldsymbol{\eta}_4} \\ 0 & 0 & ae^{i\boldsymbol{\pi}_3^\top \boldsymbol{\eta}_3} & ae^{i\boldsymbol{\pi}_3^\top \boldsymbol{\eta}_4} \end{bmatrix}$$

The product of singular values of $\boldsymbol{B}$ is

$$\sqrt{\det(\boldsymbol{B}^*\boldsymbol{B})} = 4a^3\sqrt{a^2K_1^2K_2^2 + b^2(Q_1K_2^2 + Q_2K_1^2)}, \tag{29}$$

where $Q_1 = 1 - \cos(\boldsymbol{\pi}_6^\top(\boldsymbol{\eta}_1 - \boldsymbol{\eta}_6))\cos(\boldsymbol{\pi}_1^\top(\boldsymbol{\eta}_1 - \boldsymbol{\eta}_6)), Q_2 = 1 - \cos(\boldsymbol{\pi}_6^\top(\boldsymbol{\eta}_3 - \boldsymbol{\eta}_4))\cos(\boldsymbol{\pi}_3^\top(\boldsymbol{\eta}_3 - \boldsymbol{\eta}_4)), K_1 = \sin(\boldsymbol{\pi}_1^\top(\boldsymbol{\eta}_1 - \boldsymbol{\eta}_6)), K_2 = \sin(\boldsymbol{\pi}_3^\top(\boldsymbol{\eta}_3 - \boldsymbol{\eta}_4))$.

If the previous strong orthogonal condition on $\boldsymbol{\eta}_1, \boldsymbol{\eta}_3, \boldsymbol{\eta}_4, \boldsymbol{\eta}_6$ holds, then $K_1 = K_2 = 0$ and $m_0(0) = m_0^C(0) = 0$. Therefore, the strong orthogonal condition (**c2**) cannot be satisfied at the same time. In particular, we consider the following constraints on phase $\boldsymbol{\eta}_k \in \mathbb{Z}^2$, $k = 1, \cdots, 6$:

$$\begin{aligned} &(\boldsymbol{\eta}_1 - \boldsymbol{\eta}_2)^\top(-\pi/2, \pi/2) = (\boldsymbol{\eta}_5 - \boldsymbol{\eta}_6)^\top(-\pi/2, \pi/2) = \pi \,(\mathrm{mod}\, 2\pi) \\ &(\boldsymbol{\eta}_2 - \boldsymbol{\eta}_3)^\top(\pi/2, \pi/2) = (\boldsymbol{\eta}_4 - \boldsymbol{\eta}_5)^\top(\pi/2, \pi/2) = \pi \,(\mathrm{mod}\, 2\pi) \\ &(\boldsymbol{\eta}_3 - \boldsymbol{\eta}_4)^\top(-\pi/2, \pi/2) = -\pi/2 \,(\mathrm{mod}\, 2\pi) \quad (\boldsymbol{\eta}_6 - \boldsymbol{\eta}_1)^\top(\pi/2, \pi/2) = \pi/2 \,(\mathrm{mod}\, 2\pi) \end{aligned} \tag{30}$$

where we require strong orthogonal constraints on pair of shifts corresponding to $\widetilde{m}$ function with non-diagonal common boundary and weaker constraints on $(\boldsymbol{\eta}_1, \boldsymbol{\eta}_6)$ and $(\boldsymbol{\eta}_3, \boldsymbol{\eta}_4)$. A solution to (30) is

$$\begin{aligned} &\boldsymbol{\eta}_1 = (0,0),\ \boldsymbol{\eta}_2 = (-1,1),\ \boldsymbol{\eta}_3 = (0,2), \\ &\boldsymbol{\eta}_4 = (1,0),\ \boldsymbol{\eta}_5 = (0,-1),\ \boldsymbol{\eta}_6 = (0,1). \end{aligned} \tag{31}$$

5.3 Computing m_0

Remove this sub-section, or place it after the main result on discontinuity.

Let $C_{\boldsymbol{\omega}} = det(\widetilde{\mathbf{M}}[-k_{\boldsymbol{\omega}}, :])$, then we have the following observation.

Lemma 5.11. $C_{\boldsymbol{\omega}} = C_{\boldsymbol{\omega}+\boldsymbol{\pi}_2} = C_{\boldsymbol{\omega}+\boldsymbol{\pi}_4} = C_{\boldsymbol{\omega}+\boldsymbol{\pi}_6}$

Proof Because $\widetilde{M}(\boldsymbol{\omega} + \boldsymbol{\pi}_2) = P_{\boldsymbol{\pi}_2}\widetilde{\mathbf{M}}(\boldsymbol{\omega})$ where $P_{\boldsymbol{\pi}_2}$ is a row permutation ma-

trix, it follows from the definition of $C_{\boldsymbol{\omega}}$ that $C_{\boldsymbol{\omega}} = det\big(\widetilde{\mathbf{M}}[-k_{\boldsymbol{\omega}},:](\boldsymbol{\omega})\big) = det\big(\widetilde{\mathbf{M}}[-k_{\boldsymbol{\omega}+\boldsymbol{\pi}_2},:](\boldsymbol{\omega}+\boldsymbol{\pi}_2)\big) = C_{\boldsymbol{\omega}+\boldsymbol{\pi}_2}$ where $\mathbf{1}_{k_{\boldsymbol{\omega}+\boldsymbol{\pi}_2}} = P_{\boldsymbol{\pi}_2}\mathbf{1}_{k_{\boldsymbol{\omega}}}$. □

We assume that $m_0 \in \mathbb{R}_{\geq 0}$ without phase. Let $m_0^C(\boldsymbol{\omega}) = m_0(\boldsymbol{\omega})|C_{\boldsymbol{\omega}}| \in \mathbb{R}_{\geq 0}$ and $\widetilde{m_0}^C(\boldsymbol{\omega}) = \widetilde{m_0}(\boldsymbol{\omega})/|C_{\boldsymbol{\omega}}|$, then Lemma 5.11 implies the following.

Proposition 5.12. *$m_0(\boldsymbol{\omega})$, $\widetilde{m_0}(\boldsymbol{\omega}), m_i(\boldsymbol{\omega})$, $i = 1,...,6$ satisfy (16) given $\widetilde{m_i}(\boldsymbol{\omega})$, $i = 1,...,6$ if and only if $m_0^C(\boldsymbol{\omega})$, $\widetilde{m_0}^C(\boldsymbol{\omega}), m_i(\boldsymbol{\omega})$, $i = 1,...,6$ do. More generally, $m_0^C(\boldsymbol{\omega})c(\boldsymbol{\omega})$, $\widetilde{m_0}^C(\boldsymbol{\omega})c(\boldsymbol{\omega})^{-1}, m_i(\boldsymbol{\omega})$, $i = 1,...,6$ satisfy (16) if $c(\boldsymbol{\omega}) = c(\boldsymbol{\omega}+\boldsymbol{\pi}_2) = c(\boldsymbol{\omega}+\boldsymbol{\pi}_4) = c(\boldsymbol{\omega}+\boldsymbol{\pi}_6) \neq 0$.*

According to Proposition 5.12, we can first solve $\widetilde{m_0}^C(\boldsymbol{\omega})$ and $m_0^C(\boldsymbol{\omega})$ and then construct $c(\boldsymbol{\omega})$ for optimal $\widetilde{m_0}(\boldsymbol{\omega})$ and $m_0(\boldsymbol{\omega})$. In particular, m_0^C can be computed without knowing $k_{\boldsymbol{\omega}}$,

$$m_0^C(\boldsymbol{\omega}) = m_0(\boldsymbol{\omega})|C_{\boldsymbol{\omega}}| = |det(\widetilde{\mathbf{M}}_{1,1}[-k_{\boldsymbol{\omega}},:])| = \prod_{i=1}^{6}\sigma_i(\widetilde{\mathbf{M}}_{1,1}[-k_{\boldsymbol{\omega}},:]) = \prod_{i=1}^{6}\sigma_i(\widetilde{\mathbf{M}}_{1,1}). \tag{32}$$

In practice, we first perform QR decomposition on $\widetilde{\mathbf{M}}^{\square} := \widetilde{\mathbf{M}}_{1,1}$ and then take the absolute value of the product of the diagonal entries of the upper triangular matrix, $diag(R)$. We propose the following algorithm for bi-orthogonal directional filter construction with dilated quincunx downsampling scheme:

construction of bi-orthogonal basis

Input: $\widetilde{m_i}(\boldsymbol{\omega})$, $i = 1,...,6$

1. compute $m_0^C(\boldsymbol{\omega}) = \left|det(\widetilde{\mathbf{M}}_{1,1}[-k_{\boldsymbol{\omega}},:])\right|$
2. compute $\widetilde{m_0}^C(\boldsymbol{\omega})$, such that (16) is solvable and (17) holds
3. solve $m_i(\boldsymbol{\omega})$, $i = 1,...,6$ according to (16)
4. design $c(\boldsymbol{\omega})$ and let $m_0(\boldsymbol{\omega}) = m_0^C(\boldsymbol{\omega})c(\boldsymbol{\omega})$, $\widetilde{m_0}(\boldsymbol{\omega}) = \widetilde{m_0}^C(\boldsymbol{\omega})\overline{c}(\boldsymbol{\omega})^{-1}$

5.4 solving m_i

In the final step, we substitute $\widetilde{m_0}^C(\boldsymbol{\omega})$ and $m_0^C(\boldsymbol{\omega})$ into (16) and rewrite it into the following linear system,

$$\overline{\widetilde{\mathbf{M}}}[:,2:7]\,\mathbf{m}[2:7](\boldsymbol{\omega}) = \begin{bmatrix} 1 - m_0^C\overline{\widetilde{m_0}^C}(\boldsymbol{\omega}) \\ 0 \\ -m_0^C\overline{\widetilde{m_0}^C}(\boldsymbol{\omega}+\boldsymbol{\pi}_2) \\ \vdots \\ 0 \end{bmatrix} =: \mathbf{b}(\boldsymbol{\omega}). \tag{33}$$

The solution of (33) depends only on $m_0^C\overline{\widetilde{m_0}^C}$, or equivalently $m_0\overline{\widetilde{m_0}}$.

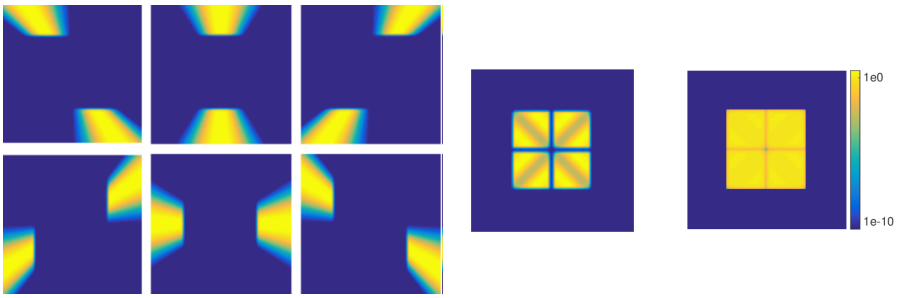

Figure 5: Left: $|\widetilde{m_i}(\boldsymbol{\omega})|$, middle: computed m_0^C, right: $\log(m_0^C)$

6 Numerical Experiments

6.1 solving m_0^C

A set of $\widetilde{m_i}(\boldsymbol{\omega})$ that satisfy the conditions of Theorem 5.8 with phase terms in (31) is used as the input of (16). The left figure in Fig.5 shows the absolute value of $\widetilde{m_i}(\boldsymbol{\omega})$. In particular, $\widetilde{m_i}(\boldsymbol{\omega}) = 0$, $\forall \omega \in S_1$. We follow the construction process in Section 5.3 and obtain m_0^C shown in the right of Fig.5, in both normal scale and log scale. We perform a numerical sanity check on the necessary condition in Proposition 5.3, that is $\forall\, \boldsymbol{\omega}$, $s.t.[m_0(\boldsymbol{\omega}), m_0(\boldsymbol{\omega}+\boldsymbol{\pi}_2), m_0(\boldsymbol{\omega}+\boldsymbol{\pi}_4), m_0(\boldsymbol{\omega}+\boldsymbol{\pi}_6)]$ is not a linear combination of the rows of $\mathfrak{D}(\boldsymbol{\omega})$ in (25). Equivalently, we compute the following quantity

$$\vartheta = 1 - \|V^\top \mathfrak{m}_0\|/\|\mathfrak{m}_0\|,$$

where $\mathfrak{m}_0(\boldsymbol{\omega}) = [m_0(\boldsymbol{\omega}), m_0(\boldsymbol{\omega}+\boldsymbol{\pi}_2), m_0(\boldsymbol{\omega}+\boldsymbol{\pi}_4), m_0(\boldsymbol{\omega}+\boldsymbol{\pi}_6)]^\top$ and V are the left singular vectors of $\mathfrak{D}(\omega)$ whose corresponding singular values are non-zero. If $\mathfrak{m}_0 \in span(V)$, then $\vartheta = 0$. If $\mathfrak{m}_0 \perp span(V)$, then $\vartheta = 1$. Fig.6 shows the feasibility check ϑ of input $\widetilde{m_i}(\boldsymbol{\omega})$, and $\mathfrak{m}_0$ is orthogonal to $span(V)$ everywhere.

6.2 solving $\widetilde{m_0}^C(\boldsymbol{\omega})$ and m_i

We compute $\widetilde{m_0}^C(\boldsymbol{\omega})$ by solving the following optimization problem similar to (22) for the dyadic scheme,

$$\min_{\mathbf{x}} \ \|\boldsymbol{D}(\mathbf{m}_0^C \circ \mathbf{x})\|^2 + \lambda \|\mathbf{w} \circ \mathbf{m}_0^C \circ \mathbf{x}\|^2, \quad s.t.\ A\mathbf{x} = \mathbf{1},\ \mathfrak{D}\mathbf{x} = \mathbf{0} \tag{34}$$

where $\circ$ is Hadamard product and $\mathbf{w}$ is a weight vector and we consider real solution $\mathbf{x}$ here. A in the constraint is the matrix generated from the identity condition (17) and $\mathfrak{D}$ is generated from the singularity condition (25). Since A and $\mathfrak{D}$ are linearly independent, (34) is feasible. Here, instead of optimizing the properties of $\mathbf{x}$ as in (22), we optimize those of $\widetilde{\mathbf{m}_0}^C \circ \mathbf{x}$ since $m_0^C \cdot \widetilde{m_0}^C$ will be later re-decomposed into m_0 and $\widetilde{m_0}$. In addition, if m_0^C is symmetric with respect to the two coordinates ω_x and ω_y, then we impose the same symmetry on $\widetilde{m_0}^C$ by solving (34) on $[0, \pi) \times [0, \pi)$ and then extend the solution to $[-\pi, \pi) \times [-\pi, \pi)$ by symmetry.

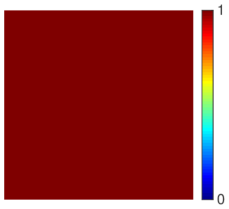

Figure 6: ϑ

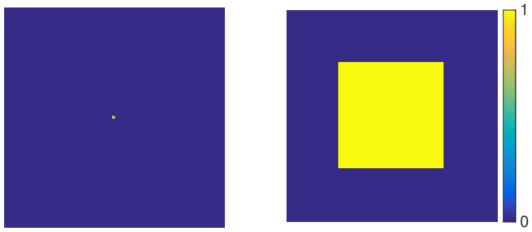

Figure 7: Left: : computed $\widetilde{m_0}^C$, right: $\widetilde{m_0}^C \cdot m_0^C$

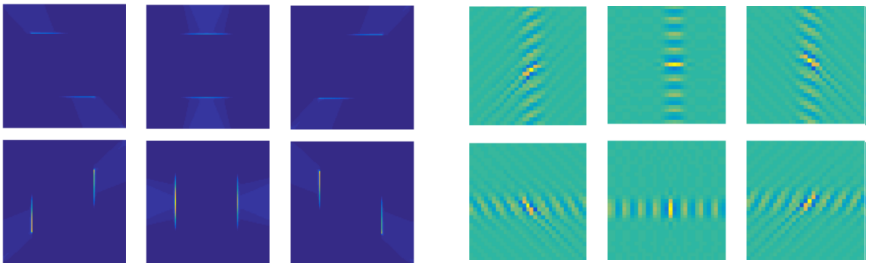

Figure 8: Left: $|m_i|$, $i = 1, \cdots, 6$, right:$|\mathcal{F}^{-1} m_i|$

Fig.7 shows $\widetilde{m_0}^C(\boldsymbol{\omega})$ obtained from (34) and $\widetilde{m_0}^C \cdot m_0^C$ which is $\mathbf{1}_{S_1}$.

In particular, given $\widetilde{m_0}^C \cdot m_0^C = 1$, $\mathbf{b}(\boldsymbol{\omega}) = \mathbf{0}$, $\forall\, \boldsymbol{\omega} \in S_1$, hence $\mathbf{m}[2:7] = \mathbf{0}$. When $\mathbf{b}(\boldsymbol{\omega}) \neq \mathbf{0}$, (33) is a degenerated over-determinant linear system (we also do a sanity check here for the linearity between $\widetilde{\overline{\mathbf{M}}}[:, 2:7]$ and $\mathbf{b}$ by computing ϑ) and

$$\mathbf{m}[2:7](\boldsymbol{\omega}) = \left(\widetilde{\overline{\mathbf{M}}}[:, 2:7]\right)^{\dagger} \mathbf{b}(\boldsymbol{\omega}),$$

where $\dagger$ is the pseudo-inverse of a matrix. Fig.8 shows the solution m_i of (33) and the corresponding spatial filters $\mathcal{F}^{-1}\widetilde{m_0}$. As shown in Fig.8, the energy of m_i concentrates on $\{|\omega_x| = \frac{\pi}{2}, |\omega_y| = \frac{\pi}{2}\}$ where $|\widetilde{m_i}|$ is small, and the filters decay slowly in time domain.

The bi-orthogonal bases constructed is not ideal, despite the regularization on m_0 in the optimization (34). Since no explicit regularization is put on m_i, it's difficult to control the regularity of the output m_i from the input $\widetilde{m_i}$.

7 Conclusion and future work

In this paper, we consider directional wavelet schemes on dilated quincunx sublattice and analyze their regularity. We show that filters in bi-orthogonal bases have the same discontinuity in the frequency domain as that of the orthonormal bases at the corners of $S_1 = [-\pi/2, \pi/2) \times [-\pi/2, \pi/2)$, hence they cannot be not well localized in the time domain.

We construct the bi-orthogonal taking a different approach from the or-

thonormal case, where directional dual filters are first designed such that they can be completed to a bi-orthogonal frame and the remaining filters are obtained by solving feasible linear systems or quadratic optimization. Its extension to low-redundancy dual frame construction is not studied here and will be our future focus.

Appendices

A Proof of Theorem 1

Take the Fourier transform of both sides of (6), we have

$$\sum_{\boldsymbol{k}}\langle f,\phi_{\boldsymbol{k}}\rangle\hat{\phi}(\boldsymbol{\omega})e^{-i\boldsymbol{\omega}^T\boldsymbol{k}}=\sum_{\boldsymbol{k}}\langle f,\phi_{1,\boldsymbol{k}}\rangle e^{-i\boldsymbol{\omega}^T\boldsymbol{D_2k}}|\boldsymbol{D_2}|^{1/2}\hat{\phi}(\boldsymbol{D_2}^T\boldsymbol{\omega})$$
$$+\sum_{j=1}^{J}\sum_{\boldsymbol{k}}\langle f,\psi^j_{1,\boldsymbol{k}}\rangle e^{-i\boldsymbol{\omega}^T\boldsymbol{Dk}}|\boldsymbol{D}|^{1/2}\hat{\phi}(\boldsymbol{D}^T\boldsymbol{\omega})$$

Suppose m_j are trigonometric series

$$m_0(\boldsymbol{\omega})=\sum_{\boldsymbol{k}}c_{\boldsymbol{k}}e^{-i\boldsymbol{\omega}^T\boldsymbol{k}}\quad m_j(\boldsymbol{\omega})=\sum_{\boldsymbol{k}}g_{\boldsymbol{k}}e^{-i\boldsymbol{\omega}^T\boldsymbol{k}},\quad j=1,\cdots,J \tag{35}$$

The first term on the right hand side can be represented by $\hat{\phi}(\boldsymbol{\omega})$ and $\langle f,\phi_k\rangle$ using (1) and (35).

$$\begin{aligned}\text{the first term on R.H.S. }&=\sum_{\boldsymbol{k}}\langle f,\phi_{1,\boldsymbol{k}}\rangle e^{-i\boldsymbol{\omega}^T\boldsymbol{D_2k}}|\boldsymbol{D_2}|^{1/2}m_0(\boldsymbol{\omega})\hat{\phi}(\boldsymbol{\omega})\\&=\sum_{\boldsymbol{k}}\Big(\sum_{\boldsymbol{k'}}\langle f,\phi_{\boldsymbol{k'}}\rangle\overline{c_{\boldsymbol{k'}-\boldsymbol{D_2k}}}|\boldsymbol{D_2}|^{1/2}\Big)e^{-i\boldsymbol{\omega}^T\boldsymbol{D_2k}}|\boldsymbol{D_2}|^{1/2}m_0(\boldsymbol{\omega})\hat{\phi}(\boldsymbol{\omega})\\&=\sum_{\boldsymbol{k'}}\langle f,\phi_{\boldsymbol{k'}}\rangle\Big(|\boldsymbol{D_2}|\sum_{\boldsymbol{k}}\overline{c_{\boldsymbol{k'}-\boldsymbol{D_2k}}}e^{i\boldsymbol{\omega}^T(\boldsymbol{k'}-\boldsymbol{D_2k})}\Big)e^{-i\boldsymbol{\omega}^T\boldsymbol{k'}}m_0(\boldsymbol{\omega})\hat{\phi}(\boldsymbol{\omega}).\end{aligned}$$

Remark. If we have a shift $\boldsymbol{k}_0$ in the down-sample scheme, i.e. $\boldsymbol{D_2}\mathbb{Z}^2-\boldsymbol{k}_0$ instead of $\boldsymbol{D_2}\mathbb{Z}^2$, so that we obtain coefficient of $\tilde{\phi}_{1,\boldsymbol{k}}=\phi_{1,\boldsymbol{k}+\boldsymbol{k}_0}$ instead of $\phi_{1,\boldsymbol{k}}$, and $\tilde{\phi}_1(\boldsymbol{x})=\phi_1(\boldsymbol{x}-\boldsymbol{k}_0)=|\boldsymbol{D_2}|^{1/2}\sum_{\boldsymbol{k}}c_{\boldsymbol{k}}\phi(\boldsymbol{x}-\boldsymbol{k}-\boldsymbol{k}_0)=|\boldsymbol{D_2}|^{1/2}\sum_{\boldsymbol{k}}c_{\boldsymbol{k}-\boldsymbol{k}_0}\phi(\boldsymbol{x}-\boldsymbol{k})$. This change of down-sample scheme results in an extra phase term $e^{-i\boldsymbol{\omega}^T\boldsymbol{k}_0}$ in m_0. Here, we use the down-sample scheme without translation.

Since $\bigcup_{\boldsymbol{\beta}\in B}\{\boldsymbol{\beta}\}:=\bigcup_{\boldsymbol{\beta}\in B}(\boldsymbol{D_2}\mathbb{Z}^2+\boldsymbol{\beta})=\mathbb{Z}^2$, where $B=\{(0,0),\,(1,0),\,(0,1),\,(1,1)\}$, the summation over $\boldsymbol{k'}\in\mathbb{Z}^2$ can be written as a double sum $\sum_{\boldsymbol{\beta}\in B}\sum_{\boldsymbol{k'}\in\{\boldsymbol{\beta}\}}$,

$$\sum_{\boldsymbol{\beta}\in B}\sum_{\boldsymbol{k'}\in\{\boldsymbol{\beta}\}}\langle f,\phi_{\boldsymbol{k'}}\rangle\sum_{\boldsymbol{k}}\overline{c_{\boldsymbol{k'}-\boldsymbol{D_2k}}}e^{i\boldsymbol{\omega}^T(\boldsymbol{k'}-\boldsymbol{D_2k})}e^{-i\boldsymbol{\omega}^T\boldsymbol{k'}}|\boldsymbol{D_2}|m_0(\boldsymbol{\omega})\hat{\phi}(\boldsymbol{\omega})$$
$$=\sum_{\boldsymbol{\beta}\in B}\sum_{\boldsymbol{k'}\in\{\boldsymbol{\beta}\}}\langle f,\phi_{\boldsymbol{k'}}\rangle\sum_{\boldsymbol{k}\in\{\boldsymbol{\beta}\}}\overline{c_{\boldsymbol{k}}}e^{i\boldsymbol{\omega}^T\boldsymbol{k}}e^{-i\boldsymbol{\omega}^T\boldsymbol{k'}}|\boldsymbol{D_2}|m_0(\boldsymbol{\omega})\hat{\phi}(\boldsymbol{\omega})$$

The summation over $\boldsymbol{k}$ in the middle is similar to the trigonometric form of m_0

in (35), but $\boldsymbol{k}$ takes value on the shifted sub-lattice $\{\boldsymbol{\beta}\}$ instead of $\mathbb{Z}^2$. Therefore, the summation equals to instead a linear combination of m_0 with shifts Γ_0,

$$\sum_{\boldsymbol{\pi}\in\Gamma_0} m_0(\boldsymbol{\omega}+\boldsymbol{\pi})\, e^{i\boldsymbol{\beta}^T\boldsymbol{\pi}} = \sum_{\boldsymbol{k}\in\{\boldsymbol{\beta}\}} c_{\boldsymbol{k}} e^{-i\boldsymbol{\omega}^T\boldsymbol{k}} \tag{36}$$

Substitute (36) into the previous expression,

$$\sum_{\boldsymbol{\beta}\in B}\sum_{\boldsymbol{k}'\in\{\boldsymbol{\beta}\}} \langle f,\phi_{\boldsymbol{k}'}\rangle \sum_{\boldsymbol{\pi}\in\Gamma_0} \overline{m_0(\boldsymbol{\omega}+\boldsymbol{\pi})}\, e^{-i\boldsymbol{\beta}^T\boldsymbol{\pi}}\, e^{-i\boldsymbol{\omega}^T\boldsymbol{k}'} m_0(\boldsymbol{\omega})\hat{\phi}(\boldsymbol{\omega})$$

Since $e^{i\boldsymbol{\pi}^T\boldsymbol{\beta}} = e^{i\boldsymbol{\pi}^T\boldsymbol{k}'}$, $\forall \boldsymbol{k}' \in \{\boldsymbol{\beta}\}$, after rewriting the double sum over $\boldsymbol{k}'$ back to a unit sum on $\mathbb{Z}^2$, we get

$$\sum_{\boldsymbol{k}'} \langle f,\phi_{\boldsymbol{k}'}\rangle e^{-i\boldsymbol{\omega}^T\boldsymbol{k}'}\hat{\phi}(\boldsymbol{\omega})\Big(\sum_{\boldsymbol{\pi}\in\Gamma_0} \overline{m_0(\boldsymbol{\omega}+\boldsymbol{\pi})} m_0(\boldsymbol{\omega}) e^{-i\boldsymbol{\pi}^T\boldsymbol{k}'}\Big)$$

Similarly, the second term on the R.H.S. of (6) equals to

$$\sum_{j=1}^{J}\sum_{\boldsymbol{k}'} \langle f,\phi_{\boldsymbol{k}'}\rangle e^{-i\boldsymbol{\omega}^T\boldsymbol{k}'}\hat{\phi}(\boldsymbol{\omega})\Big(\sum_{\boldsymbol{\pi}\in\Gamma_1} \overline{m_j(\boldsymbol{\omega}+\boldsymbol{\pi})} m_j(\boldsymbol{\omega}) e^{-i\boldsymbol{\pi}^T\boldsymbol{k}'}\Big)$$

(For Theorem 3 on frame construction, the summation of shifts $\boldsymbol{\pi}$ is over Γ_0 instead of Γ_1.) Combining the two terms on the R.H.S. of (6), and compare the coefficients of $\langle f,\phi_{\boldsymbol{k}'}\rangle e^{-i\boldsymbol{\omega}^T\boldsymbol{k}'}\hat{\phi}(\boldsymbol{\omega})$ on both sides, the perfect reconstruction condition is then equivalent to $\forall \boldsymbol{k}'$,

$$\sum_{\boldsymbol{\pi}\in\Gamma_0} e^{-i\boldsymbol{\pi}^T\boldsymbol{k}'}\overline{m_0(\boldsymbol{\omega}+\boldsymbol{\pi})} m_0(\boldsymbol{\omega}) + \sum_j \sum_{\boldsymbol{\pi}\in\Gamma_1} e^{-i\boldsymbol{\pi}^T\boldsymbol{k}'}\overline{m_j(\boldsymbol{\omega}+\boldsymbol{\pi})} m_j(\boldsymbol{\omega}) = 1.$$

This is equivalent to

$$|m_0(\boldsymbol{\omega})|^2 + \sum_j |m_j(\boldsymbol{\omega})|^2 = 1$$

and

$$\sum_{j=0}^{J} \overline{m_j(\boldsymbol{\omega}+\boldsymbol{\pi})} m_j(\boldsymbol{\omega}) = 0,\ \boldsymbol{\pi}\in\Gamma_0\setminus\{\mathbf{0}\}$$

$$\sum_{j=1}^{J} \overline{m_j(\boldsymbol{\omega}+\boldsymbol{\pi})} m_j(\boldsymbol{\omega}) = 0,\ \boldsymbol{\pi}\in\Gamma_1\setminus\Gamma_0$$

Remark. Because each m_j is $(2\pi, 2\pi)$ periodic, we only need to check the above equality $\forall \boldsymbol{\omega}\in S_0$. If we downsample ψ_1^j on a shifted sub-lattice $\boldsymbol{D}\mathbb{Z}^2 - \boldsymbol{k}_j$, we then have an extra phase $e^{i\boldsymbol{\pi}^T\boldsymbol{k}_j}$ before $\overline{m_j(\boldsymbol{\omega}+\boldsymbol{\pi})} m_j(\boldsymbol{\omega})$ in shift cancellation condition. This provides additional freedom in the construction yet it is not substantial.

B Supplementary Numerical Results

B.1 Numerical optimization of $\widetilde{m_0}(\boldsymbol{\omega})$ in 1D

To test whether numerical optimization is a practical way to solve (20), we first experiment on $m_0(\omega)$ and $\widetilde{m_0}(\boldsymbol{\omega})$ of pre-designed bi-orthogonal wavelets. We

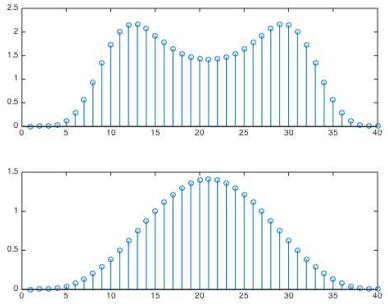

Figure 10: $m_0(\boldsymbol{\omega})$ and $\widetilde{m_0}(\boldsymbol{\omega})$

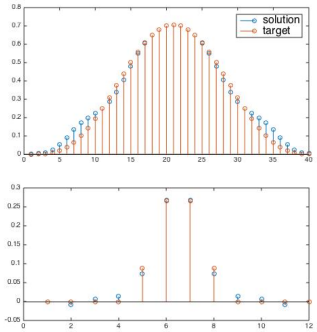

Figure 11: $\widehat{\widetilde{m_0}}(\boldsymbol{\omega})$ vs. $\widetilde{m_0}(\boldsymbol{\omega})$

consider a low frequency filters corresponding to bi-orthogonal scaling functions ϕ, $\tilde{\phi}$ with vanishing moments 3 and 5 respectively.

The filters are shown in Fig.9. Suppose we know the upper decomposition filter, and we want to find the lower reconstruction filter by solving (20), such that the filter has support as compact as possible. The corresponding m_0 and $\widetilde{m_0}$ are complex, yet we can shift the phase of m_0 such that m_0 is real and apply the same phase shift to $\widetilde{m_0}(\boldsymbol{\omega})$. Without loss of generality, (20) can be solved assuming that m_0 is real. It is not necessary that the corredponding $\widetilde{m_0}$ is also real, but in this testing case, $m_0(\boldsymbol{\omega})$ and $\widetilde{m_0}(\boldsymbol{\omega})$ have the same phase, hence the phase-shifted $\widetilde{m_0}(\boldsymbol{\omega})$ is real as well. Fig.10 shows the ground truth $m_0(\boldsymbol{\omega})$ and $\widetilde{m_0}(\boldsymbol{\omega})$ considered in this simulation.

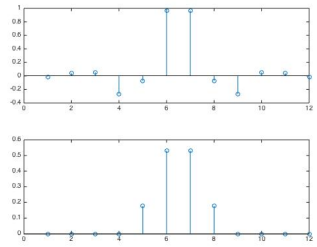

Figure 9: 1d filters, up: LoD, down: LoR

Let $\widehat{\widetilde{m_0}}(\boldsymbol{\omega})$ be the approximation of $\widetilde{m_0}(\boldsymbol{\omega})$, which is solution of the following optimization problem

$$\min_{\mathbf{x}} \|\boldsymbol{D}\mathbf{x}\|^2 + \|\mathbf{x}\|^2, \quad s.t.\ \boldsymbol{A}\mathbf{x} = \mathbf{1} \tag{37}$$

where $\boldsymbol{A}$ in the constraint is the matrix generated from (17) (in 1D, only a single shift of π appears in the condition, so each row of $\boldsymbol{A}$ has two non-zero entries). Notice that no symmetry constraint is imposed here, nevertheless, the solution shown in Fig.11 is almost symmetric. On the other hand, its support in the time domain is not as compact as that of $\widetilde{m_0}(\boldsymbol{\omega})$, see the bottom of Fig.11.

B.2 Numerical optimization of $\widetilde{m_0}(\boldsymbol{\omega})$ in 2D

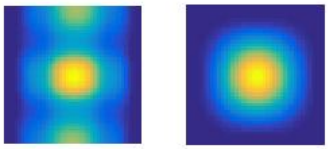

Figure 12: Left: result of (37) in 2D, Right: target

The 2D case is much harder and several different optimization problems are formulated and their solutions are shown in the following. The 2D bi-orthogonal low-pass filters used here are the tensor products of the 1D filters used above.

2D version of (37)

The 1D formulation can be easily extended to 2D, where $\boldsymbol{D} = [\boldsymbol{D}_x, \boldsymbol{D}_y]$ consider 1st order derivative in both x and y directions, and $\boldsymbol{A}$ is generated from (17), each row has four non-zero entries. Fig.12 shows the minimizer and compares it with the target function. It is obvious that the solution is not 90°-rotation invariant. Even worse is the fact that there is much energy in the vertical high-frequency domain.

To enforce the support of $\widehat{\widetilde{m_0}}(\boldsymbol{\omega})$ concentrates within the low frequency domain, the squared ℓ_2-norm regulator in (37) is changed to a weighted version (corresponding to Modulation space) as follows,

$$\min_{\mathbf{x}} \ \|\boldsymbol{D}\mathbf{x}\|^2 + \lambda\|\mathbf{w} \circ \mathbf{x}\|^2, \quad s.t.\ \boldsymbol{A}\mathbf{x} = \mathbf{1} \tag{38}$$

where $\circ$ is Hadamard product and $\mathbf{w}$ is a weight vector. In particular, we choose $\forall\omega,\ \mathbf{w}(\boldsymbol{\omega}) = \|\boldsymbol{\omega}\|$. Fig.13 and Fig.14 show the minimizer of (38) with $\lambda = 60$ and 600 respectively. As λ increases, the support of the minimizer concentrates more within the low frequency region. As shown in Fig.13, when λ is not huge, the minimizer achieves a certain level of but not full symmetry, whereas Fig.14 shows that huge λ imposes full symmetry.

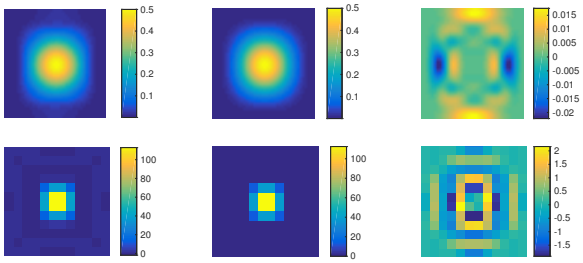

Figure 13: result of (38) $\widehat{\widetilde{m_0}}(\boldsymbol{\omega})$ ($\lambda = 60$), target $\widehat{\widetilde{m_0}}(\boldsymbol{\omega})$ and their difference, Top: frequency domain, Bottom: time domain

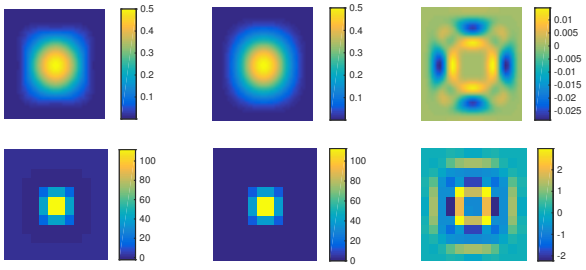

Figure 14: result of (38) $\widehat{\widetilde{m_0}}(\boldsymbol{\omega})$ ($\lambda = 600$), target $\widehat{\widetilde{m_0}}(\boldsymbol{\omega})$ and their difference

weighted L2 norm with symmetry constraint
If we hard constrain the symmetry by the following

$$\min_{\mathbf{x}} \ \|\boldsymbol{D}\mathbf{x}\|^2 + \lambda\|\mathbf{w} \circ \mathbf{x}\|^2, \quad s.t.\ \boldsymbol{A}\mathbf{x} = \mathbf{1},\ \boldsymbol{S}\mathbf{x} = \mathbf{0} \tag{39}$$

where each row of $\boldsymbol{S}$ has an one entry and a negative one entry at the location of two points have the same value due to symmetry. In practice, we put symmetry constraints such that the upper half plane is symmetric to the lower half plane w.r.t. x coordinate and the first quadrant is $90°-$ rotational invariant w.r.t. the second quadrant. The symmetry constraint makes the optimization problem significantly harder, resulting in longer optimization algorithm running time and no near-optimal solution is found (the algorithm terminates as the maximum number of iterations is exceeded). Fig.15 shows the result provided by the Matlab quadratic minimization solver, unfortunately, there are artifacts at the near endpoints of x and y coordinates.
On the other hand, asymmetric solution can always be symmetrized by the average of the solution and its dual w.r.t. rotation, mirroring, etc. This approach increase the support of the solution, thus a well concentrated solution in the frequency domain is necessary to begin with.

Other potential formulations

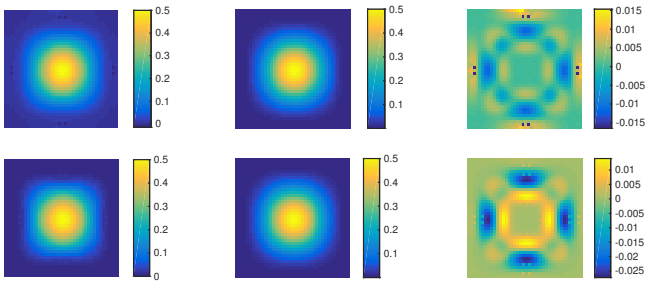

Figure 15: solution of (39) (top: $\lambda = 60$, bottom: $\lambda = 600$) provided by Matlab solver `quadprog`

We may also putting weights in the first L2-norm of derivatives, such that

$$\min_{\mathbf{x}} \ \|\mathbf{w}' \circ \boldsymbol{D}\mathbf{x}\|^2 + \lambda\|\mathbf{w} \circ \mathbf{x}\|^2, \quad s.t.\ \boldsymbol{A}\mathbf{x} = \mathbf{1} \tag{40}$$

Clearly, $\mathbf{w}'(\boldsymbol{\omega}) \to +\infty$ as $|\boldsymbol{\omega}| \to +\infty$, but its behavior near the origin is unclear.

References

[1] R. H. Bamberger and M. J. T. Smith, "A filter bank for the directional decomposition of images: theory and design," *IEEE Transactions on Signal Processing*, vol. 40, no. 4, pp. 882–893, Apr 1992.

[2] T. T. Nguyen and S. Oraintara, "Multiresolution direction filterbanks: theory, design, and applications," *IEEE Transactions on Signal Processing*, vol. 53, no. 10, pp. 3895–3905, Oct 2005.

[3] M. N. Do and M. Vetterli, "The contourlet transform: an efficient directional multiresolution image representation," *Image Processing, IEEE Transactions on*, vol. 14, no. 12, pp. 2091–2106, 2005.

[4] T. Sauer, "Shearlet multiresolution and multiple refinement." Kutyniok, Gitta (ed.) et al., Shearlets. Multiscale analysis for multivariate data. Boston, MA: Birkhäuser. Applied and Numerical Harmonic Analysis, 199-237 (2012)., 2012.

[5] G. Easley, D. Labate, and W.-Q. Lim, "Sparse directional image representations using the discrete shearlet transform," *Applied and Computational Harmonic Analysis*, vol. 25, no. 1, pp. 25–46, 2008.

[6] E. Candes, L. Demanet, D. Donoho, and L. Ying, "Fast discrete curvelet transforms," *Multiscale Modeling & Simulation*, vol. 5, no. 3, pp. 861–899, 2006.

[7] I. W. Selesnick, R. G. Baraniuk, and N. C. Kingsbury, "The dual-tree complex wavelet transform," *Signal Processing Magazine, IEEE*, vol. 22, no. 6, pp. 123–151, 2005.

[8] S. Durand, "M-band filtering and nonredundant directional wavelets," *Applied and Computational Harmonic Analysis*, vol. 22, no. 1, pp. 124 – 139, 2007.

[9] R. Yin, "Construction of orthonormal directional wavelets based on quincunx dilation subsampling," in *Sampling Theory and Applications (SampTA), 2015 International Conference on*, May 2015, pp. 292–296.

[10] A. Cohen and J.-M. Schlenker, "Compactly supported bidimensional wavelet bases with hexagonal symmetry," *Constructive approximation*, vol. 9, no. 2-3, pp. 209–236, 1993.

[11] A. Cohen, I. Daubechies, and J.-C. Feauveau, "Biorthogonal bases of compactly supported wavelets," *Communications on pure and applied mathematics*, vol. 45, no. 5, pp. 485–560, 1992.